



# Asynchronous Holocene optimum of the East Asian monsoon

Zhisheng An<sup>a</sup>, Stephen C. Porter<sup>a,b,\*</sup>, John E. Kutzbach<sup>c</sup>, Wu Xihao<sup>d</sup>, Wang Suming<sup>e</sup>,  
Liu Xiaodong<sup>f</sup>, Li Xiaoqiang<sup>a</sup>, Zhou Weijian<sup>a</sup>

<sup>a</sup>*Xi'an Laboratory of Loess and Quaternary Geology, Academia Sinica, People's Republic of China*

<sup>b</sup>*Quaternary Research Center, University of Washington, Seattle, WA 98195-1360 USA*

<sup>c</sup>*Center for Climatic Research, University of Wisconsin, Madison, WI 53706 USA*

<sup>d</sup>*Institute of Geomechanics, Ministry of Geology and Mineral Resources, People's Republic of China*

<sup>e</sup>*Nanjing Institute of Geography and Lakes, Academia Sinica, People's Republic of China*

<sup>f</sup>*Lanzhou Institute of Plateau Atmosphere-Physics, Academic Sinica, People's Republic of China*

## Abstract

The spatial and temporal distribution of summer monsoon precipitation (or effective moisture) during the Holocene has been reconstructed on the basis of geological data, including lake levels, pollen profiles, and loess/paleosol records. In addition, the summer (July) precipitation increment, effective precipitation, and monsoon strength index have been obtained from numerical modeling experiments. Both geological data and numerical modeling indicate that the Holocene optimum, as defined by peak East Asian summer monsoon precipitation, was asynchronous in central and eastern China, reaching a maximum at different times in different regions, e.g., ca. 10,000–8000 yr ago in northeastern China, 10,000–7000 yr ago in north-central and northern east-central China, ca. 7000–5000 yr ago in the middle and lower reaches of the Yangtze River, and ca. 3000 yr ago in southern China. In southwestern China the maximum appeared ca. 11,000 yr ago, but probably was related to the maximum landward extension of the Indian summer monsoon. The regional shift in the maximum precipitation belt from northwest to southeast over the past 10,000 yr is interpreted as a response to changing seasonality related to orbital forcing of the climate. The southeastward shift of the East Asian summer monsoon maximum is consistent with the progressive weakening of the summer monsoon as the summer solar radiation anomaly decreased progressively through the Holocene and the East Asian monsoon index declined, while the early maximum in southwestern China matches the maximum of the Indian monsoon index. © 2000 Elsevier Science Ltd. All rights reserved.

## 1. Introduction

The Asian monsoon is an important component of atmospheric circulation and plays a significant role in the global hydrologic and energy cycles. It has influenced significantly the geographic environment of the region it affects directly, as well as its marginal zones. The monsoon region of eastern China differs from other dry, subtropical, and temperate areas of the same latitudes in being densely populated. Not only is the livelihood of the people closely linked to the summer monsoon precipitation in agricultural regions, but the monsoon rains also generate devastating floods that can impact tens of thousands of people.

A critical question facing the people living in monsoonal regions is whether, and how, a rapid and significant change in global climate might affect the monsoon system. The past history of monsoon climates is important in answering this question, for it can provide evidence of the past behavior of the monsoons at times when global climate was different from what it is now, and it can provide insights about the nature and regional impacts of future changes in climate.

In the present study, we have synthesized a large body of geologic information related to changes in monsoon climate in China during the Holocene Period, and have compared the data with results from numerical experiments with a Global Climate Model that span the same time interval. The results of the two approaches are consistent, and imply that the zone of peak rainfall conditions associated with the East Asian summer monsoon shifted latitudinally across China during the Holocene in response to natural variations in solar radiation.

\* Corresponding author. Tel.: 001-206-543-1166.

E-mail address: scporter@u.washington.edu (S.C. Porter).

## 2. Monsoon climate of China

Modern climatological research has shown that the Asian monsoon system has three relatively independent subsystems, namely the Indian monsoon, the East Asian monsoon, and the Plateau monsoon (Tao and Chen, 1987; Tang, 1979). Among these, the East Asian monsoon is the dominant influence on the climate and environment of central and eastern China (Gao et al., 1962).

### 2.1. East Asian monsoon

During the seasonal transition from winter to summer, the East Asian summer monsoon moves gradually northward as Northern Hemisphere insolation increases, causing a strengthening of the thermal contrast between the warmer Asian continent and the colder Pacific Ocean. This leads to a marked pressure gradient between the ocean and land. In mid-summer, the East Asian summer monsoon advances to a ca. 40°N, spreading across the eastern part of northwestern China, northern China, and most of northeastern China.

Precipitation associated with the East Asian monsoon is produced by the interaction along the monsoon front of northward-moving moist summer monsoon air and a northern mass of cooler air. Usually, the belt of heavy monsoon rainfall consists of somewhat discontinuous rain bands that form as the front moves northward. The rainfall belt migrates with the frontal system, leading to asynchronous onset of summer monsoon precipitation in different areas. The rain belt is stable when the front maintains a quasi-stationary state. The first pause occurs in the second week of May in the maritime areas of southern China. The second pause occurs in the third week of June in areas between the Yangtze and Yellow rivers. The third pause, in mid-July, occurs in northern and northeastern China.

Rain belt changes are characterized by their abruptness, for they occur in sudden jumps in response to insolation-induced general circulation changes in East Asia (Gao et al., 1962; Lau et al., 1988). This situation contrasts with the Indian monsoon rainfall regime, which is caused by convection of moist, unstable air flowing northward from the intertropical convergence zone (Ramage, 1987). Consequently, the region of the Chinese monsoon is among the most complicated and unique climatic regions of the world. Judging from geologic records, the Asian monsoon system has developed during the late Cenozoic (e.g., Ruddiman and Kutzbach, 1991; Sun et al., 1998).

Precipitation ( $P$ ) variability is more important than evaporation ( $E$ ) variability for understanding the variation in effective moisture ( $P-E$ ) in the East Asian monsoon region. Between the southern (Guangzhou) and the northern (Harbin) regions of central and eastern China the difference in annual average temperature is more

than 18°C and the difference in annual average precipitation is about 1100 mm (Zhang and Lin, 1985). However, the difference in annual average evaporation is generally no more than 700 mm between these two regions because the lower temperature in northern China generally decreases evaporation and the higher relative humidity of southern China results in a decrease in evaporation under the higher-temperature conditions (Zhang and Lin, 1985).

Kutzbach and Guetter (1986) and COHMAP Members (1988) modeled the variation of tropical monsoon climate since the last glaciation in northern Africa and southern Asia. They showed that the monsoon systems of these regions varied systematically in response to variations in solar insolation related to changes in the Earth's orbital parameters. An et al. (1990a, 1991b) studied the evolution of the East Asian monsoon over the last 20,000 and 130,000 yr, respectively. The variation of the monsoon climate in China is not just a response to external orbital forcing; it also is related to such factors as the configuration of sea and land (An et al., 1991b), the uplift of the Qinghai-Xizang (Tibetan) Plateau (Ruddiman and Kutzbach, 1991), the distribution of high-latitude and high-altitude ice and snow, and sea-surface temperature (Porter and An, 1995).

### 2.2. The Holocene optimum

Considerable attention has been directed to the history of Chinese monsoon climate (e.g., Zhou et al., 1984; Li and Liang, 1985; Xia, 1988; Liu, 1989; Yang, 1989; Sun and Yuan, 1990; An et al., 1990b; Shi et al., 1992). Of significance to this history is the Holocene optimum, not only because it was an important recent climatic episode, and produced a varied array of geologic records, but also because it might serve as an important analog for future climatic change in this region. The Holocene (or climatic) optimum is often regarded as the time of maximum postglacial warmth (e.g., Winkler and Wang, 1993). It also has been defined informally as “the postglacial interval of most equable climate, with warm temperatures and abundant rainfall” (Bates and Jackson, 1987). In using the term, a single parameter (e.g., mean annual or seasonal temperature, or precipitation) often is not specified. Nevertheless, the concept is derived from the mid-Holocene Atlantic interval of the northern European pollen stratigraphy, which was characterized by a warm and generally moist climate. Recognized as globally diachronous, it is not generally considered a time-stratigraphic entity.

Quite different opinions have been expressed as to the time of the Holocene optimum in different parts of China, defined mainly on the basis of postglacial temperature variations. Its onset has been variously placed at 10,000–7500 yr BP and its end at 5000–2000 yr BP. However, both precipitation and effective moisture are

considered important environmental parameters within the region of the East Asian monsoon (i.e., in central and eastern China), and are closely related to changes in winter and summer monsoon intensity. Furthermore, many of the available high-resolution paleoclimate proxy records can be interpreted in terms of precipitation or effective moisture variations, rather than temperature. Accordingly, in this paper we treat the Holocene optimum in China as a precipitation (or effective moisture) maximum, without reference to temperature, and will argue that it is a time-transgressive phenomenon (i.e., not a chronostratigraphic unit).

### 3. Paleoenvironmental data and modeling

We have divided central and eastern China into six regions (A–F), based on physiography, taking into account the horizontal resolution of the numerical model used in this study (Fig. 1 Table 1); region G in western China, a vast area with a relative paucity of information, includes the Qinghai-Xizang (Tibetan) Plateau. Geologic data, such as lake-level records, lacustrine and swamp deposits, pollen-spore sequences, and the magnetic susceptibility of loess-paleosol sequences, are used to recon-

struct past precipitation or effective moisture during the last 12,000 yr. Numerical modeling, using the CCM0 (Community Climate Model 0 of the US National Center for Atmospheric Research; Pitcher et al., 1983; Kutzbach and Guetter, 1986), is used to obtain estimates of summer (July) precipitation, effective precipitation, and the monsoon strength index. The modeling results are then compared with the geologic climate-proxy evidence.

#### 3.1. Lake-level fluctuations

Lake levels constitute a sensitive index of hydrological climate, especially as a measure of the effective humidity of a region, and can be determined by analyzing paleoshoreline features, sedimentary facies, and fossils (Street-Perrott and Harrison, 1984). Data available for regions A, B + C, D, and F are plotted in 3000-yr intervals in Fig. 2 (region E is omitted from the plot due to lack of adequate paleolacustrine sedimentary profiles). Lake-level status is reported as high, middle, or low (= large, intermediate, or small area, following Street and Grove (1979), and is defined as follows: high/large =  $\geq 70\%$  of the highest level/largest area; intermediate status = 20–70% of highest level/largest area; and low/small =  $\leq 20\%$  of highest level/largest area.

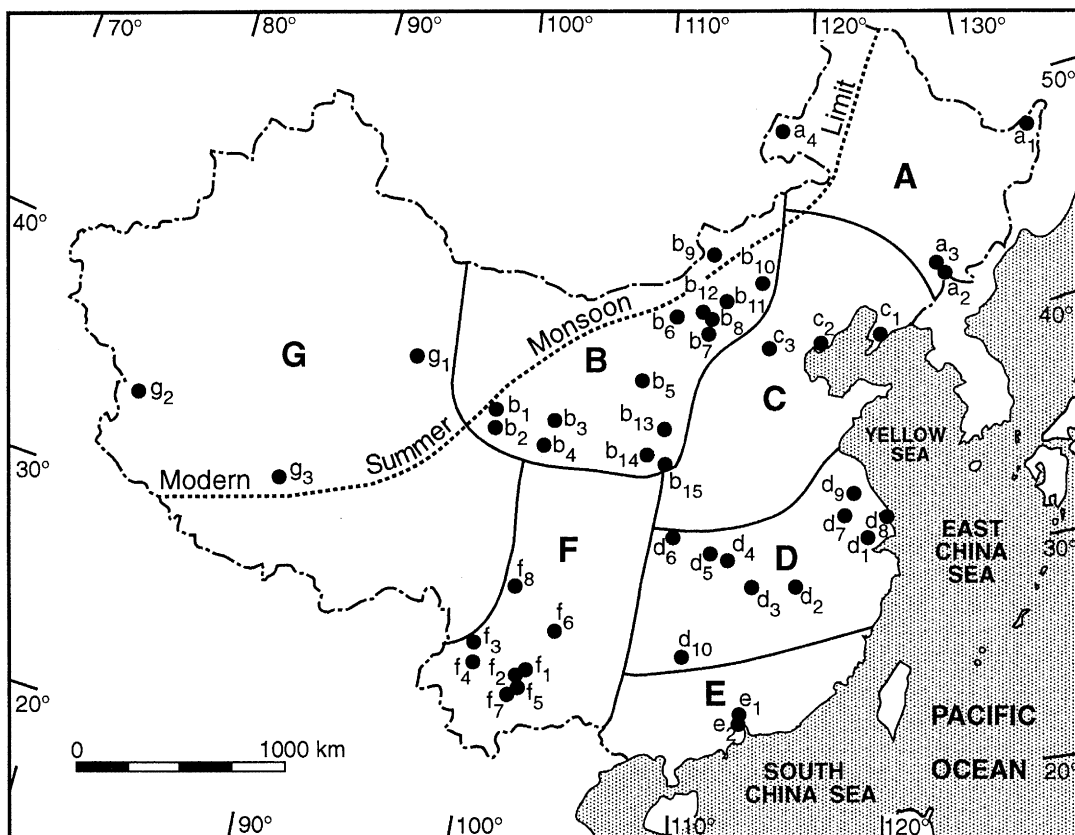


Fig. 1. Map of China showing subdivisions of the Chinese monsoon region based on physiography and numerical modeling, and the locations of the geological records analyzed (Table 1). Landward limit of modern summer monsoon front is after Gao (1962).

Table 1  
Locations and altitudes of Holocene paleoclimatic proxy sites

Site #	Name	N Latitude	E Longitude	Altitude (m)
<i>A Northeastern China</i>				
a <sub>1</sub>	Qingdeli	48°00'	133°15'	52
a <sub>2</sub>	Jingchuan	42°20'	126°22'	600
a <sub>3</sub>	Gushantong	42°30'	126°10'	600
a <sub>4</sub>	Hulong Lake	49°00'	117°20'	540
<i>B North-central China</i>				
b <sub>1</sub>	Qinghai Lake	37°10'	100°00'	3165
b <sub>2</sub>	Halali	36°40'	99°53'	3220
b <sub>3</sub>	Jiuzhoutai	36°05'	103°48'	2060
b <sub>4</sub>	Baxie	35°34'	103°35'	2000
b <sub>5</sub>	Salawusu	37°50'	108°40'	1400
b <sub>6</sub>	Wudangzhao	40°50'	110°15'	1200
b <sub>7</sub>	Daihai Lake	40°35'	112°40'	1260
b <sub>8</sub>	Huangqihai	40°50'	113°15'	1264
b <sub>9</sub>	Chaganlimenoer	43°16'	112°53'	1060
b <sub>10</sub>	Dalainoer	43°20'	116°40'	1230
b <sub>11</sub>	Chanhanzhao	41°30'	113°52'	1270
b <sub>12</sub>	Baisuhai	41°08'	112°40'	2000
b <sub>13</sub>	Luochuan	35°44'	109°25'	1010
b <sub>14</sub>	Fuping	34°50'	109°50'	500
b <sub>15</sub>	Beizhuangcun	34°22'	109°32'	520
<i>C. Northern east-central China</i>				
c <sub>1</sub>	Pulandian	39°30'	112°00'	20
c <sub>2</sub>	Maohebei	39°32'	119°12'	2
c <sub>3</sub>	Baiyandian	38°50'	116°00'	20
<i>D. Middle and lower reaches of the Yangtze River</i>				
d <sub>1</sub>	Taihu Lake	30°55'–31°35'	119°50'–120°35'	3
d <sub>2</sub>	Poyang Lake	28°30'–29°40'	115°50'–116°40'	8
d <sub>3</sub>	Dongting Lake	28°40'–29°30'	111°45'–113°10'	10
d <sub>4</sub>	Guyuanmence	29°40'–30°20'	111°40'–112°25'	15
d <sub>5</sub>	Longquan Lake	30°53'	111°52'	50
d <sub>6</sub>	Dajiu Lake	31°25'	110°10'	2500
d <sub>7</sub>	Zhengjiang	32°12'	119°25'	15
d <sub>8</sub>	Qidong	31°50'	121°40'	2
d <sub>9</sub>	Jianhu	33°30'	119°45'	10
d <sub>10</sub>	Daping	26°10'	110°10'	1640
<i>E. Southeastern China</i>				
e <sub>1</sub>	Huangsha	23°10'	110°20'	6
e <sub>2</sub>	Fangyu	22°55'	113°25'	2
<i>F. Southwestern China</i>				
f <sub>1</sub>	Dianchi Lake	24°40'–25°03'	102°35'–40'	1886
f <sub>2</sub>	Caohai Lake	25°00'	112°40'	1890
f <sub>3</sub>	Eryuan	26°08'	99°55'	2050
f <sub>4</sub>	Erhai Lake	25°35'–55'	110°08'–15'	1980
f <sub>5</sub>	Fuxian Lake	24°25'–35'	102°50'–55'	1720
f <sub>6</sub>	Caohai Lake (Weining)	26°50'	104°12'	2220
f <sub>7</sub>	Jimenghai	24°10'	102°45'	1500
f <sub>8</sub>	Mianning	28°40'	102°20'	2400
<i>G. Qinghai-Xizang (Tibetan) Plateau</i>				
g <sub>1</sub>	Daqaidan	37°50'	95°15'	3000
g <sub>2</sub>	Sumxi Co	34°18'	80°08'	5058
g <sub>3</sub>	Seling Co	31°34'–37'	88°31'–89°21'	4530

Region A (northeastern China) is mainly characterized by an interconnected system of Holocene lakes and swamps that drain externally, but are sensitive to climatic

change (Harrison and Digerfeldt, 1993). Four lakes, Gushantun of Jilin (Liu, 1989), Jingchuan (Sun and Yuan, 1990), Qindeli of Heilongjiang (Xia, 1988), and Hulonghu

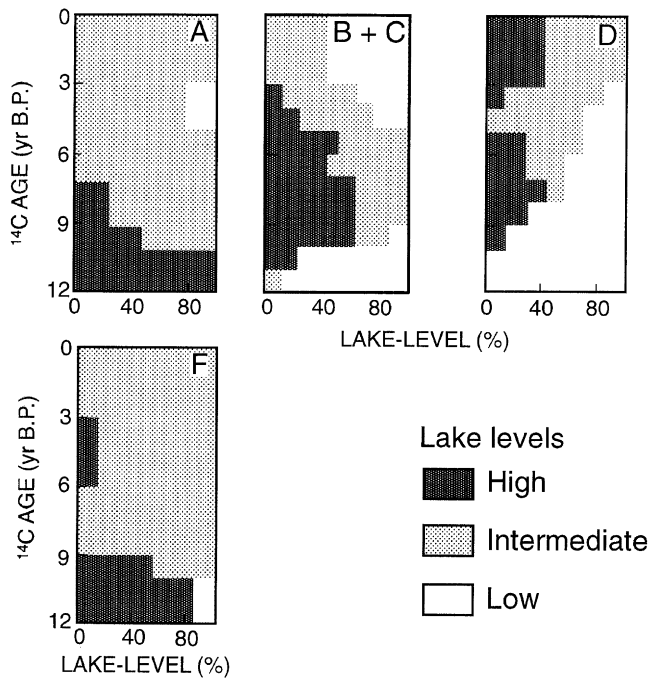


Fig. 2. Temporal variation in percentage of lakes with high, intermediate or low level. Region A: lakes  $a_1$ ,  $a_2$ ,  $a_3$ ,  $a_4$  in Fig. 1; region B + C north to the Yellow River: lakes  $b_5$ ,  $b_7$ ,  $b_8$ ,  $b_9$ ,  $b_{10}$ ,  $b_{11}$ ,  $b_{12}$ ,  $c_1$ ,  $c_3$ ; region D: lakes  $d_1$ – $d_7$ ; region F: lakes  $f_1$ – $f_7$ . Chronology of all lake records is based on conventional, uncalibrated  $^{14}\text{C}$  dating.

of Inner Mongolia (Wang et al., 1994), have been analyzed on the basis of changing sedimentary facies and fossil remains in lake or swamp deposits (Xue and Wang, 1994). The data show that all lakes with adequate records were high from 12,000–10,000 yr BP, and that the percentage of lakes with high levels decreased to ca. 50% from 10,000–9,000 yr BP and to ca. 25% from 9,000–7,000 yr BP. No post-7,000 yr BP high lake stages have been recorded; for this period intermediate levels dominated. Thus, lakes were deepest and most extensive before 10,000 yr BP when summer monsoon precipitation (and, locally, meltwater from thawing permafrost) apparently was high and/or the evaporation rate was low because of relatively low temperatures towards the end of the last glaciation.

In regions B + C (central northern and eastern central China), most lakes do not discharge and can be viewed as “natural precipitation gauges”. Nine lakes have been analyzed [i.e.,  $b_5$  (Yuan, 1988),  $b_7$  (Wang et al., 1990a,b),  $b_8$  (Li et al., 1992a),  $b_9$  (Sun, 1990),  $b_{11}$  (Geng, 1988; Li, 1992),  $b_{12}$  (Cui and Kong, 1992),  $c_1$  (Institute of Geochemistry, 1977), and  $c_3$  (Xu et al., 1988)]. High lake levels began to appear ca. 11,000 yr BP (22%) and prevailed from 10,000–7,000 yr BP (60%). Since 5,000 yr BP, intermediate and low levels were dominant, and since 3,000 yr BP low levels have prevailed.

In the middle and lower reaches of the Yangtze River (region D, Fig. 1), lakes are hydrologically connected with rivers, and lake-level fluctuations have been controlled not only by local precipitation but also by stream runoff, including ice and snow melt in stream source areas. Seven lakes were analyzed [ $d_1$  (Sun and Wu, 1987a),  $d_2$  (Editorial Committee of a Studies on Poyang Lake, 1987),  $d_3$  (Zhang, 1991),  $d_4$  (Tan, 1980),  $d_5$  (Li et al., 1992a),  $d_6$  (Li et al., 1992b), and  $d_7$  (Xu and Zhu, 1984)]. Although high lake levels have never dominated the region as a whole, there are two periods when they were most prevalent, i.e., 8,000–7,000 and 3,000–0 yr BP. The first period is inferred to have been related to a precipitation increase, whereas the second was largely related to a decline in the evaporation rate due to lower temperatures and persistence of the summer monsoon front in the region.

In region F (southwestern China), lakes are found near stream divides and often have restricted outlets. As a result of their semi-confined character, the lakes are sensitive to precipitation. Seven lakes have been analyzed;  $f_1$  (Zhu, 1989),  $f_2$  (Zhou et al., 1992),  $f_3$ – $f_5$  (Lin, 1987; Song, 1994),  $f_6$  (Lin and Zheng, 1987), and  $f_7$  (Nanjing Institute of Geography and Limnology, CAS, 1989). About 84% of the lakes were high from 12,000–10,000 yr BP, but only 56% were high from 10,000–9,000 yr BP. Since 9,000 yr BP, intermediate lake levels were dominant, with only a brief interval between 6,000 and 3,000 yr BP when one lake was high, possibly related to strengthening of the Indian summer monsoon.

### 3.2. Pollen analyses

More than 100 published pollen profiles have been reviewed in this study. Representative diagrams with  $^{14}\text{C}$  control are presented for each of the six regions shown in Fig. 1 as proxy records of precipitation, effective moisture, or relative summer monsoon strength.

In the East Asian monsoon region of China, modern vegetation zonation is largely related to precipitation, especially summer monsoon precipitation, and to temperature. From north and south, the principal vegetation zones are as follows: mixed-needle deciduous broadleaf forests and deciduous broadleaf forests in the temperate zone; deciduous broadleaf forests (containing evergreen broadleaf components); mixed evergreen broadleaf and deciduous broadleaf forests in the northern and middle subtropical zone; and monsoon evergreen broadleaf forests in the southern subtropical zone (Wu et al. 1980; Liu, 1988). The deciduous broadleaf forest component of the northern and middle subtropical zone and the monsoon evergreen broadleaf and rain-forest components of the southern subtropical zone are closely related to summer rainfall. Therefore, these components can be viewed as indicators of monsoonal rainfall conditions.

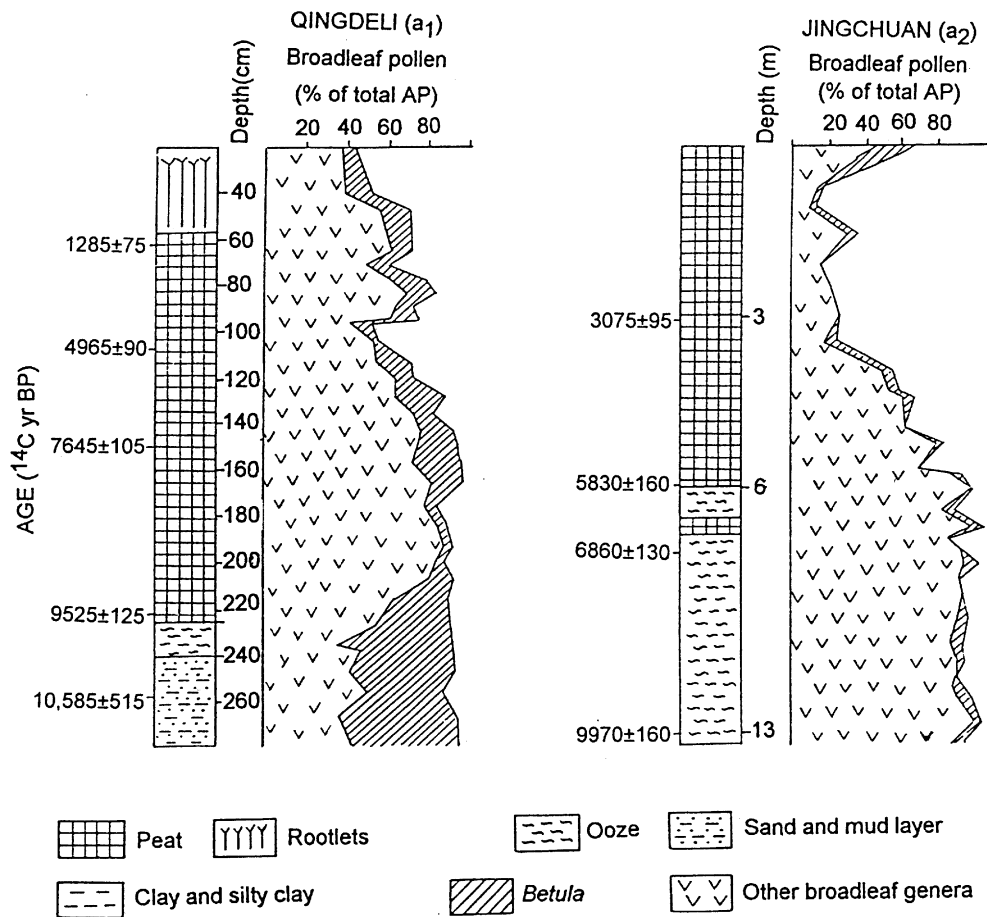


Fig. 3. Percentage of deciduous broad-leaf pollen in the arboreal (AP) total, northeastern China. Qingdeli (a<sub>1</sub>): *Ulmus*, *Quercus*, *Salix*, *Carpinus*, *Tilia*, *Acer*, *Juglans*, *Alnus*, *Corylus*. Jingchuan (a<sub>2</sub>): *Ulmus*, *Quercus*, *Salix*, *Carpinus*, *Tilia*, *Juglans*, *Corylus*, *Fraxinus*.

### 3.2.1. Northeastern China (region A)

The Qingdeli profile (a<sub>1</sub>, Fig. 3) is located in the northern part of the middle temperate zone of humid climate in a region of deciduous broadleaf forest. Representative genera include *Ulmus*, *Quercus*, *Salix*, *Carpinus*, *Tilia*, *Acer*, *Juglans*, *Alnus*, and *Betula* (the latter indicated by shading in Fig. 3). The curve of broadleaf genera plus *Betula* is high (80–90%) from 11,000 to 6000 yr BP, indicating a high effective humidity during the growing season for this interval. Omitting *Betula*, the curve shows a steep rise about 10,000 yr BP, indicating a significant strengthening of the summer monsoon. Most of the *Betula* pollen are of small size, indicating shrub birch rather than tree birch. Wu (1980) has pointed out that shrub birch requires ecological conditions characteristic of the eastern part of northeastern China, which are marked by high precipitation, high humidity, and relatively low temperature.

*Betula*, a pioneer of the broadleaf genera, appears earlier than 11,000 yr BP, indicating that humidity had reached the high values favorable for this genus during the final phase of the last glaciation, likely the result of

high precipitation and a low evaporation rate related to low mean temperatures. A similar increase in *Betula* ca. 11,000 yr BP has also been observed in the Gushantun profile (Liu, 1989). The Jingchuan profile (Fig. 3, a<sub>2</sub>) has a similar pattern, with a steady high in broadleaf pollen (*Quercus*, *Ulmus*, and *Juglans*) since at least 10,000 yr BP. Thus, an interval of high humidity (i.e., high effective moisture) can be identified that lasted from ca. 10,000 to 6000 yr BP.

### 3.2.2. North-central China (region B)

The Qinghai Lake profile (Du et al., 1989; Kelts et al., 1989; Liu and Qiu, 1994) (Fig. 4, b<sub>1</sub>) is from drill core QH85-14C, collected from the western part of Qinghai Lake. This site lies on the northeastern Qinghai-Xizang Plateau and within the plateau temperate semi-dry grassland at the margin of the East Asian monsoon region. The climate of Qinghai Lake is sensitive to summer monsoon variations. Because the deciduous broadleaf forest is sustained by conditions of high precipitation and summer temperature, it can be considered representative of summer monsoon conditions in the temperate zone

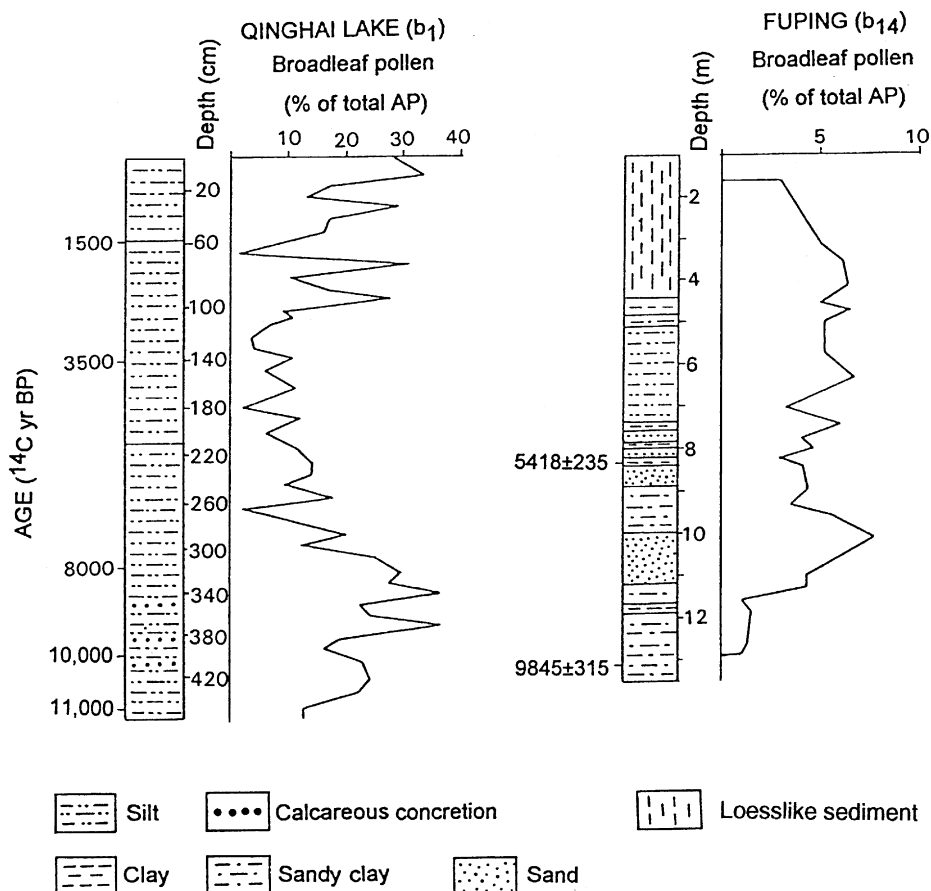


Fig. 4. Percentage of deciduous and broad-leaf pollen in the total AP in northwestern China. Qinghai Lake (b<sub>1</sub>): *Quercus*, *Betula*. Fuping (b<sub>14</sub>): *Betula*, *Corylus*, *Carpinus*, *Quercus*, *Ulmus*, *Celtis*, *Juglans*, *Ailanthus*.

(Wu, 1980). We therefore use the deciduous broadleaf components as a proxy for summer monsoon precipitation. The curve has two prominent peaks at ca. 9500 and 8500 yr BP (37%) and a rather persistent low from 8000 to 3000 yr BP. Subsequently, the percentage of deciduous broadleaf pollen (woody plants) rose to 30%, although possibly as a result of human activity.

The Jingbian profile (Li, 1991), located at the northern margin of the Loess Plateau, displays a similar pattern, with the arboreal pollen content and concentration of charcoal fragments reaching a maximum ca. 9000 yr BP.

The Fuping profile (Fig. 4, b<sub>14</sub>; Sun and Zhao, 1991) displays a broadleaf pollen peak at ca. 7000–8000 yr BP.

### 3.2.3. Northern east-central China (region C)

The Maohebei profile (Fig. 5, c<sub>2</sub>; Li and Liang, 1985) is located on the northeastern margin of the North China Plain, close to Bohai Bay. The site lies in the warm temperate zone, with semi-humid climate, and the vegetation is a deciduous broadleaf forest. The broadleaf pollen genera identified are *Quercus*, *Tilia*, *Ulmus*, *Carpinus*, *Juglans*, and *Betula*. The two peaks (ca. 20–33%) at ca. 10,000 and 8500 yr BP shown in Fig. 5 correspond to

humid periods, and the subsequent interval of lower percentages (< 15%) corresponds to a dry interval.

The Baiyangdian profile (Fig. 5, c<sub>3</sub>; Xu et al., 1988) displays a similar pattern, i.e., an abrupt increase in deciduous broadleaf pollen ca. 11,000 yr BP, with high percentages until ca. 9000 yr BP.

### 3.2.4. Middle and lower reaches of the Yangtze River (region D)

The Qidong profile (Fig. 6, d<sub>8</sub>; Liu et al., 1992) is located north of the Yangtze River mouth in the northern subtropical zone of wet climate. The vegetation is characterized by a mix of subtropical evergreen broadleaf genera and a deciduous broadleaf assemblage. Pollen genera include subtropical hygrophilic and thermophilic evergreen broadleaf *Cyclobalanopsis* and *Castanopsis*, and deciduous *Carya*. Because of inconsistent <sup>14</sup>C ages between ca. 25 and 35 m depth, the dates of 8320 ± 170 and 4460 ± 90 yr BP are used in plotting the curve. High values in the pollen concentration curve occur in the middle portion of this silty clayey section, with the highest peak at about 5000 yr BP (up to 2900 grains/cm<sup>3</sup>).

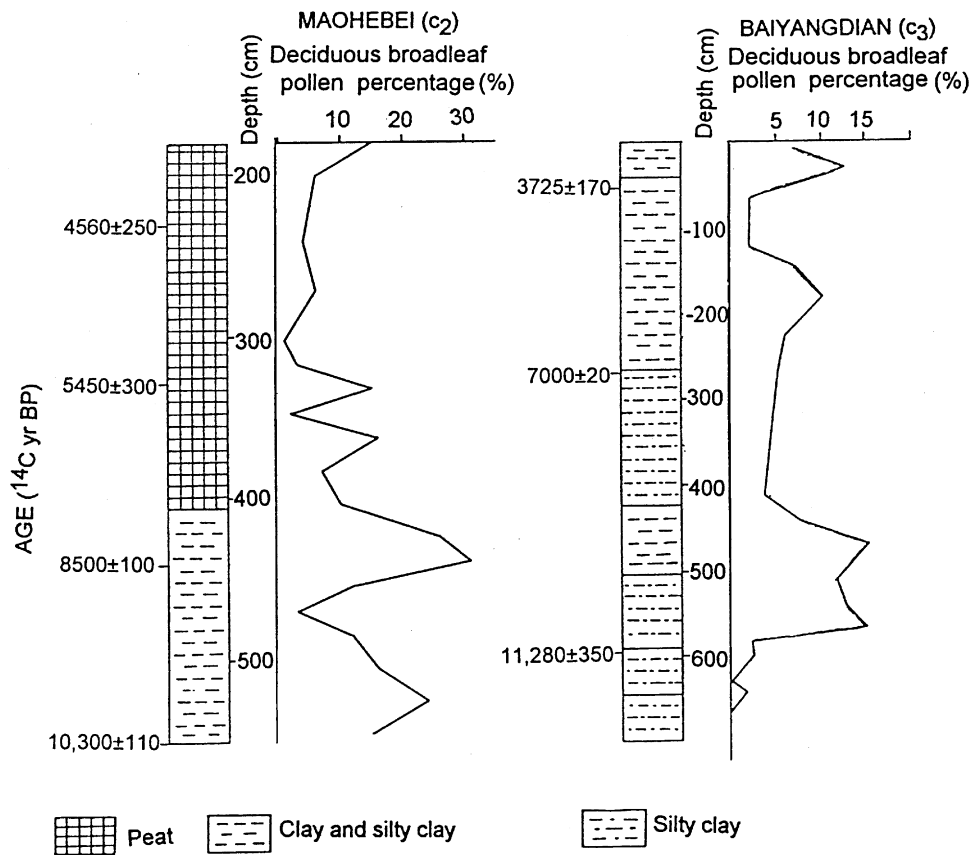


Fig. 5. Percentage of Holocene deciduous broad leaf pollen in AP total, northern China. Maohebei (c<sub>2</sub>): *Quercus*, *Tilia*, *Ulmus*, *Carpinus*, *Juglans*. Baiyangdian (c<sub>3</sub>): *Quercus*, *Tilia*, *Juglans*, *Ailanthus*, *Salix*.

The Jianhu profile (Fig. 6, d<sub>9</sub>; Tang and Shen, 1992) is located north of the Yangtze River near the Yellow Sea in the northern subtropical zone. High influx of evergreen broadleaf pollen (*Castanopsis*, *Cyclobalanopsis*, and *Quercus*; Tang and Shen, 1992; Tang et al., 1993) indicates that two humidity maxima occurred about 6700–6000 yr BP.

The Daping profile (Fig. 6, d<sub>10</sub>; Wang Jian, personal communication, 1991) lies in a zone between the middle and southern subtropical zones and is characterized by the evergreen broadleaf assemblage. At present, this is the only profile available for this region, which is important bioclimatically and geographically. The evergreen broadleaf genera in the profile are *Cyclobalanopsis*, *Castanopsis*, *Myrica*, *Magnolia*, *Elaeocarpus*, and the deciduous genus *Carya*. The inferred chronology is based on interpolation, using the average sedimentation rate of the upper 1.1 m. The curve displays a high of > 15% from ca. 7000–4000 yr BP. The peak value (> 20%) occurs at ca. 4300 yr BP.

### 3.2.5. Southern China (region E)

The Huangsha profile (Fig. 7, e<sub>1</sub>; Li et al., 1991) is located in a suburb of Guangzhou on the northern part of the Pearl River delta where the vegetation is a south-

ern subtropical evergreen broadleaf assemblage with evergreen rain forest of transitional type. The genera counted in the percentage diagram are *Elaeocarpus*, *Quercus*, *Chamionii*, *Altingia*, Apocynaceae, and Moraceae. The curve displays a broad high from ca. 5000 to 1600 yr B.P. but the three maxima at ca. 4000, 3000, and 2000 yr BP may represent times of greatest effective precipitation.

The Fanyu profile (Fig. 7, e<sub>2</sub>; Li et al., 1991) displays abundant evergreen broadleaf genera, but has its high-frequency variability lacks any clear trends. The most prominent peak at ca. 3000–2500 yr BP is apparently correlative with that in the Huangsha profile. Distinctive tropical rainforest components (i.e., *Terminalia*) and subtropical components (*Syzygium*) appear from 3500–2500 yr BP.

### 3.2.6. Southwestern China (region F)

The Eryuan profile (Fig. 8, f<sub>3</sub>; Lin, 1987) is located north of Erhai Lake in the western part of the Yunnan-Guizhou Plateau, where the climate is strongly controlled by the southwest (Indian) monsoon. The vegetation is the evergreen broadleaf assemblage of the middle subtropics. Genera represented in the pollen include

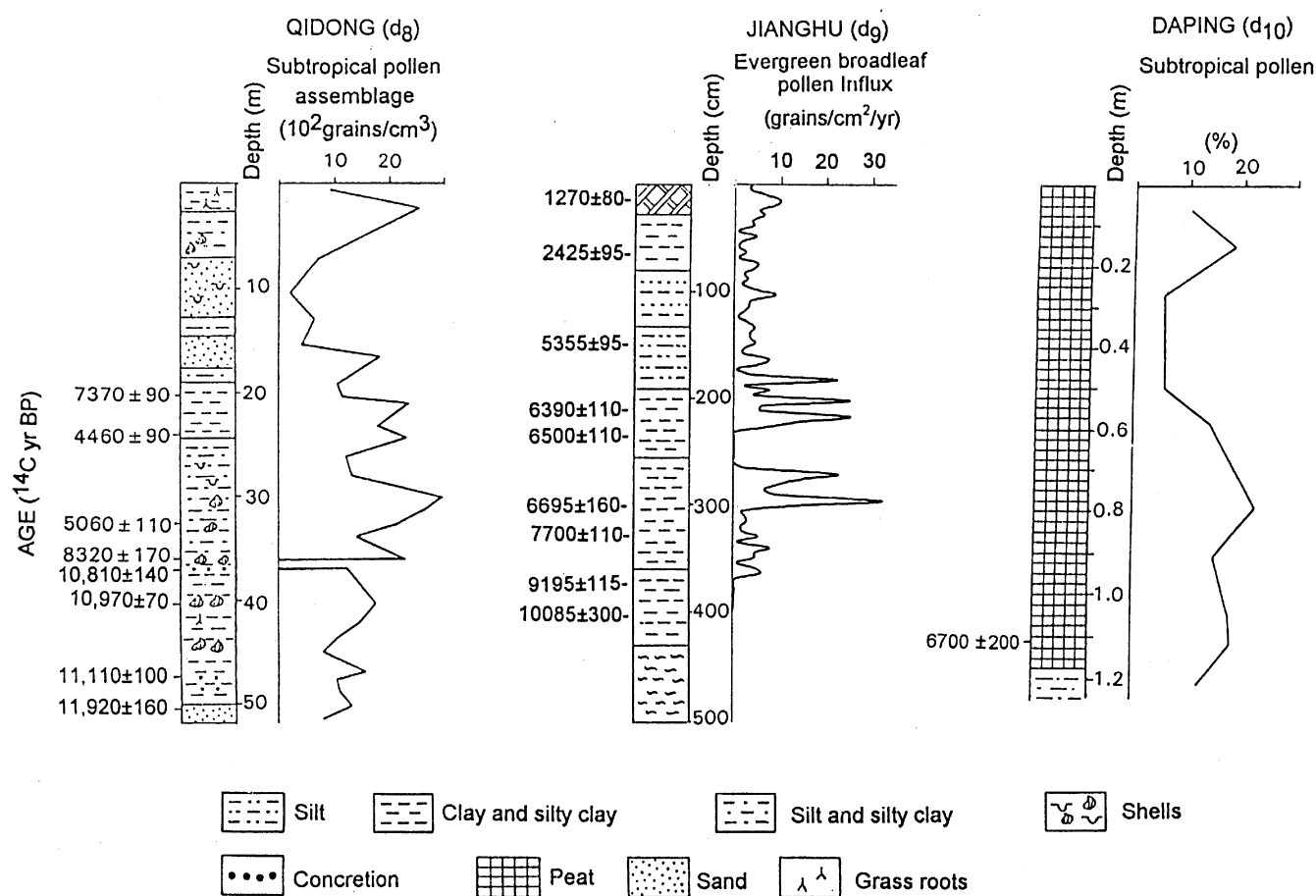


Fig. 6. Pollen concentration, pollen influx, and percentage of subtropical tree species in the middle-lower reaches of the Yangtze River. Qidong (d<sub>g</sub>): *Castanopsis*, *Cyclobalanopsis*, *Carya*. Jianghu (d<sub>g</sub>): *Castanea*, *Castanopsis*, *Quercus*. Daping (d<sub>10</sub>): *Castanopsis*, *Myrica*, *Magnolia*, *Elaeocarpus*, *Carya*.

deciduous *Quercus*, *Ulmus*, and coniferous *Tsuga*. The pollen concentration curve displays peaks at ca. 11,000 and 9200 yr B.P. (2290 and 3860 grains/cm<sup>3</sup>, respectively), indicating low temperature but a high effective humidity during the growing season. The percentage of broadleaf genera in the pollen curve of the Dianchi Lake profile (D218 drill core) increases at 13,000 yr B.P. and reaches a maximum between 10,000 and 8000 yr BP that is related to an interval of high humidity (Sun and Wu, 1987b).

Cold-resistant species dominate the vegetation between 11,000 and 9100 yr BP in a pollen profile (Fig. 8, f<sub>8</sub>; Jarvis, 1993) obtained for a core from Shayema Lake, located 15 km northeast of Mianning County (Fig. 1). Between ca. 9100 and 7800 yr BP, deciduous *Quercus* declined and evergreen *Quercus* and *Tsuga* along with other hygrophilic species increased, marking a transition to a warm, moist period.

### 3.2.7. Qinghai-Xizang (Tibetan) Plateau (region G)

Three lacustrine profiles on the Qinghai-Xizang (Tibetan) Plateau are of special interest: Daqaidan (g1)

on the northern part of the plateau (Huang et al., 1980), Sumxi Co (g2) in the west (Gasse et al., 1991), and Seling Co (g3) in the central part (Gu et al., 1993) (Figs. 1 and 9). Changes in sedimentary facies in the Daqaidan section, in <sup>18</sup>O records of the Seling Co section, and in the *Artemisia*/*Chenopodiaceae* ratio of the Sumxi Co section indicate that a rapid change in lake conditions occurred close to 10,000 yr BP during the glacial/interglacial transition. Different proxy indicators suggest that effective humidity peaked ca. 10,000–8000 yr BP and was associated with a rapid rise in temperature on the plateau at the end of the last glaciation when a decrease in snow and ice cover may have helped strengthen the summer monsoon.

### 3.3. Eolian Deposits

Since the last glaciation, eolian deposition has occurred across a broad area in China, including northeastern China, north-central China, and the middle and lower reaches of the Yangtze River, but the best developed and most thoroughly studied region is north-central China.

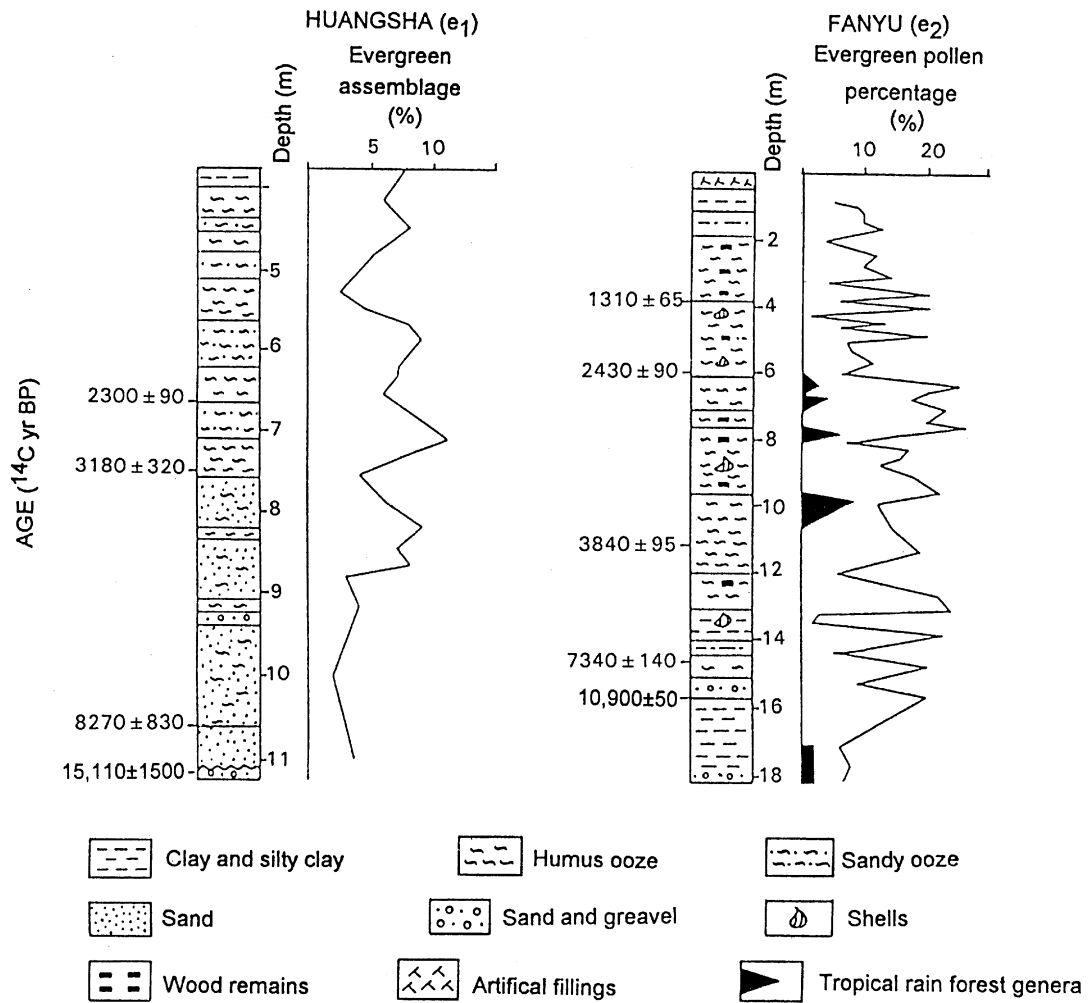


Fig. 7. Evergreen tree pollen characterizing the southern China subtropical and tropical zone. Huangsha ( $e_1$ ): *Elaeocarpus*, *Altingia*, *Apocyanaceae*, *Piperaceae*, *Palmae*, *Moraceae*. Fanyu ( $e_2$ ): *Elaeocarpus*, *Piperaceae*, *Palmae*, *Moraceae*, *Cesgtrum*, *Germinalia*.

The arid, semi-arid, and semi-humid parts of north-central China coincide with the Loess Plateau and include a border zone between desert and loess-covered terrain. Five loess-paleosol (or sand-paleosol-alluvial) profiles are shown here (Fig. 10): Halali ( $b_2$ ; Chen et al., 1991a) to the south of Qinghai Lake, Jiuzhoutai ( $b_3$ ; Chen et al., 1991b) in Lanzhou, Salawusu ( $b_5$ ) in Inner Mongolia, Wudangzhao ( $b_6$ ; Cui and Song, 1992) near the Daqing Mountains in Inner Mongolia, and Luochuan ( $b_{13}$ ; Zhou and An, 1991) on the central Loess Plateau. Generally speaking, the loess units reflect a strengthening of the winter monsoon and weakening of summer monsoon, while the paleosols represent the opposite conditions (An et al., 1991a). All five profiles contain a paleosol with basal  $^{14}\text{C}$  ages of ca. 10,000–10,700 yr BP that denotes an abrupt transition from the dry climate of the last glaciation to stronger summer monsoon conditions (a rise in effective moisture) of the early Holocene.

The magnetic susceptibility of the loess-paleosol sequence is a proxy index for the effective moisture and summer monsoon strength (An et al., 1991a). Two high-resolution susceptibility curves for the Baxie and Beizhuancun profiles provide evidence of early Holocene summer monsoon conditions.

The Baxie profile (Fig. 11,  $b_4$ ; An et al., 1993) is located at the southwestern margin of the Loess Plateau, near the northern base of the Qingling Mountains. The site is in the semi-arid warm temperate zone of forest/grassland vegetation. A palaeosol that developed from 9500–5500 yr BP, an interval corresponding to the Holocene optimum, contains two SUS peaks at ca. 9000 and 8000 yr BP (ages estimated by interpolation using a sedimentation rate based on bounding  $^{14}\text{C}$  ages) that are inferred to indicate times of maximum effective humidity and the strongest summer monsoon conditions.

The Beizhuancun (Weinan) profile (Fig. 11,  $b_{15}$ ; Zhou and An, 1991) is located at the southeastern margin of the

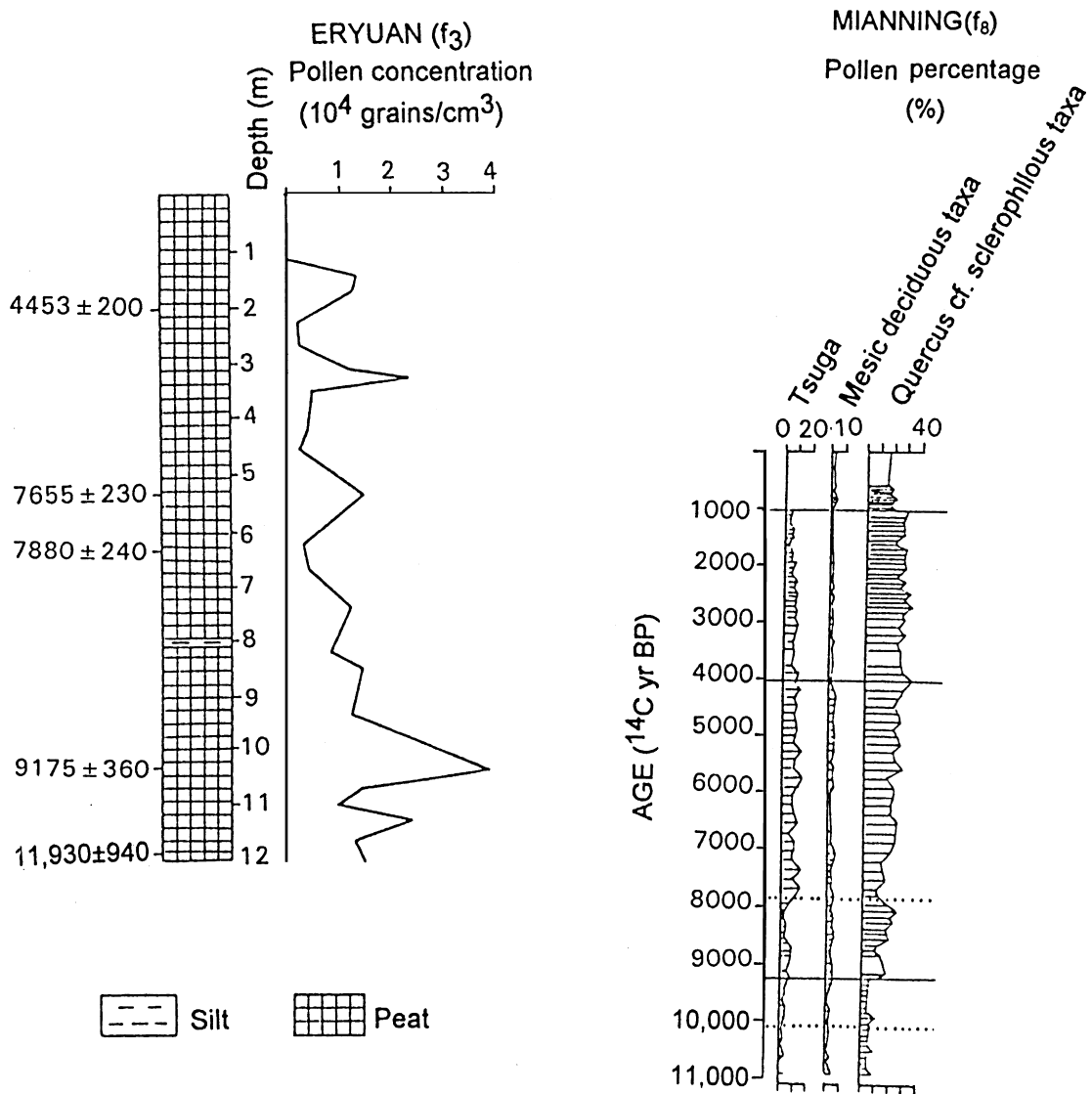


Fig. 8. Arboreal-pollen curves of humidity-sensitive genera in Southwestern China. Eryuan (f<sub>3</sub>): *Tsuga*, *Quercus*, *Ulmus*. Mianning (f<sub>8</sub>): *Tsuga*, *Mesic deciduous taxa*, *Quercus cf. sclerophyllous taxa*.

Loess Plateau at the northern foot of the Qingling Mountains in a region of semi-humid warm temperate climate with a deciduous broadleaf forest. Two paleosols developed between 9500 and 3000 yr BP. A magnetic susceptibility peak (150 SI units) at ca. 9500–8000 yr BP represents the time of maximum effective moisture.

#### 4. Numerical modeling

A series of numerical modeling simulations spanning the last 18,000 yr has been run using the CCM0 (Community Climate Model 0 of the US National Center for Atmospheric Research; Pitcher et al., 1983). CCM0 is a global three-dimensional model of atmospheric circulation, with a horizontal rhomboidal truncation of 15

waves in the east-west direction and corresponding to a horizontal resolution of 4.4° latitude × 7.5° longitude; the model has nine vertical levels. Included in the model are solar and terrestrial radiation, cumulus convection, precipitation, and evaporation. Surface temperature is calculated using a local energy balance equation. The orbital parameters, atmospheric trace-gas amounts, sea-surface temperatures, sea-ice limits, snow cover, albedo of the land surface, effective soil moisture, and surface topography (including ice sheets) are specified using available data (Williamson, 1983; Pitcher et al., 1983; Kutzbach and Guetter, 1986).

In order to analyze the variation in summer climate of eastern Asia, experiments were run for “permanent” July conditions at intervals of 3000 yr, beginning 18,000 astronomical years ago. In addition to the global results of

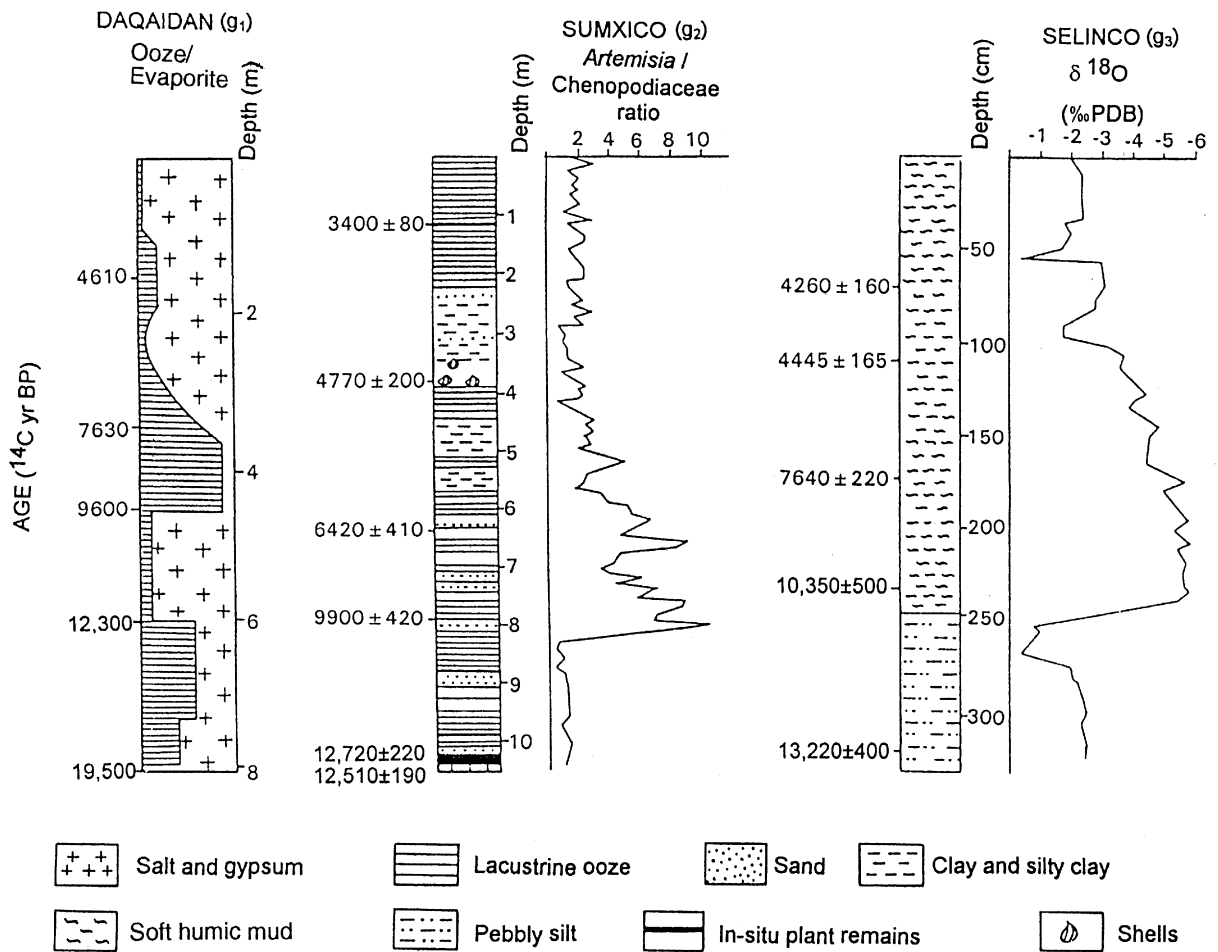


Fig. 9. Sedimentary sequences in the semi-arid and arid areas of western China.

Kutzbach and Guetter (1986), special attention has been paid to the climate of the Chinese monsoon region and neighboring areas. Modeling of modern conditions produced results that generally agree with observed sea-level air pressure, the wind field at high and low levels, air temperature, and precipitation. However, a systematic northward deviation of the model output compared with present conditions can be seen in connection with the East Asian summer monsoon system and associated rain belt. Perhaps this deviation is due to the altitude specified in the model for the Qinghai-Xizang Plateau being ca. 1500–2000 m too low. Nevertheless, this has little effect on our relative correlations of the different experiments, each of which displays similar deviations.

In our modeling, the summer precipitation maximum (deviation from the control simulation mean, in percent) for the last 15,000 yr is as follows (Fig. 12 and Table 2b): the maximum appeared at ca. 12,000 astronomical yr BP in northeastern China (region A; 23%), at 9000 yr BP in north-central and northern east-central China (regions B and C; 33 and 12%, respectively), at 6000 yr BP in the middle and lower reaches of the Yangtze River (region D;

25%), and at 3000 yr BP in southern China (region E; 12%). In southwestern China (region F), the maximum appeared early at ca. 12,000 yr BP (24%). The amplitude of the percentage deviation also differs among regions; the largest is in north-central China in the arid to semi-arid areas, whereas the smallest is in northern east-central China and southern China, beyond the northern and southern limits, respectively, of the modern “plum-rain” region. The deviation reached a minimum of  $-19\%$  at 6000 yr BP in northern east-central China, and  $-10\%$  in southwestern China at 3000 yr BP. Because the effective precipitation (moisture) is not the same as precipitation, and evaporation increases as temperature rises, the effective precipitation was also modeled, but the results were very similar.

## 5. Comparison of geologic records and numerical modeling results

Table 2 lists the times of maximum precipitation or effective moisture recorded in different regions by

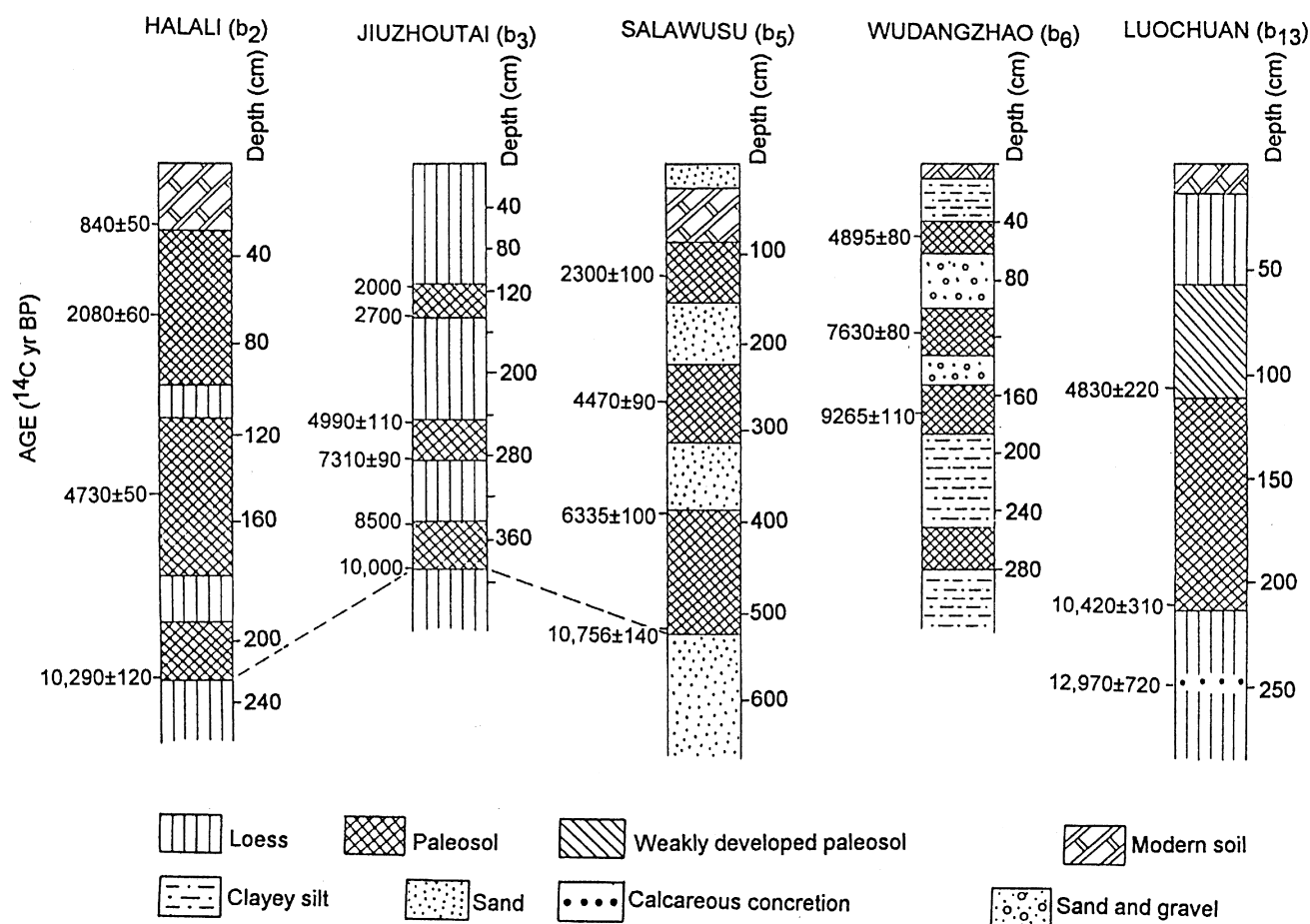


Fig. 10. Loess and paleosol profiles on the Loess Plateau.

paleoecological, paleolimnological, or geologic data and those simulated by CCM0. The  $^{14}\text{C}$  ages have been calibrated using the calibration program of Stuiver and Reimer (1993) so that the geologic records and modeling results can be compared using the same (calendric) time scale. The geologic records and modeling results are in general agreement (Figs. 13 and 14, Table 2), and show a clear diachronism in the culmination of the Holocene optimum (i.e., based on a precipitation or effective moisture maximum): it appears earlier in the north and northwest and, with the exception of southwestern China, occurs later toward the south and southeast.

The greatest precipitation recorded by the geologic data and calculated by numerical modeling in northeastern China (region A) occurred ca 12,000 cal yr BP (ca 10,300  $^{14}\text{C}$  yr BP). Air temperature toward the end of the last glaciation was relatively low, implying diminished evaporation. The rising soil humidity would have been increasingly favorable for the establishment of the deciduous broadleaf assemblage. By contrast, in southern China (region E) the amplitude of the variation of precipitation since the last glaciation calculated by modeling

has been relatively small, in agreement with pollen data that display only a minor peak and some increase in the rainforest component.

Whereas the ranges in calibrated ages for lake-level and pollen data in the northern regions of China are broadly comparable or overlap, for those in the southern regions the maximum effective precipitation recorded by lake-level fluctuations apparently occurred somewhat earlier than that recorded by pollen data. Possibly this reflects a quicker response of lake levels to changes in precipitation, whereas a slower response of vegetation resulted in a detectable lag.

In most regions, the time of greatest precipitation calculated by numerical modeling is comparable to that recorded by geologic data. Apparent discrepancies in a few cases (e.g., middle-lower Yangtze River) could be caused either by the arbitrary 3000-yr time resolution of the model, by climatic boundary conditions that were selected a priori for the model, or by model deficiencies. It should be noted, however, that the horizontal resolution of CCM0 is not adequate for simulating shifts of monsoon precipitation on the scale of several hundred kilometers. The six regions (Figs. 1 and 12) are

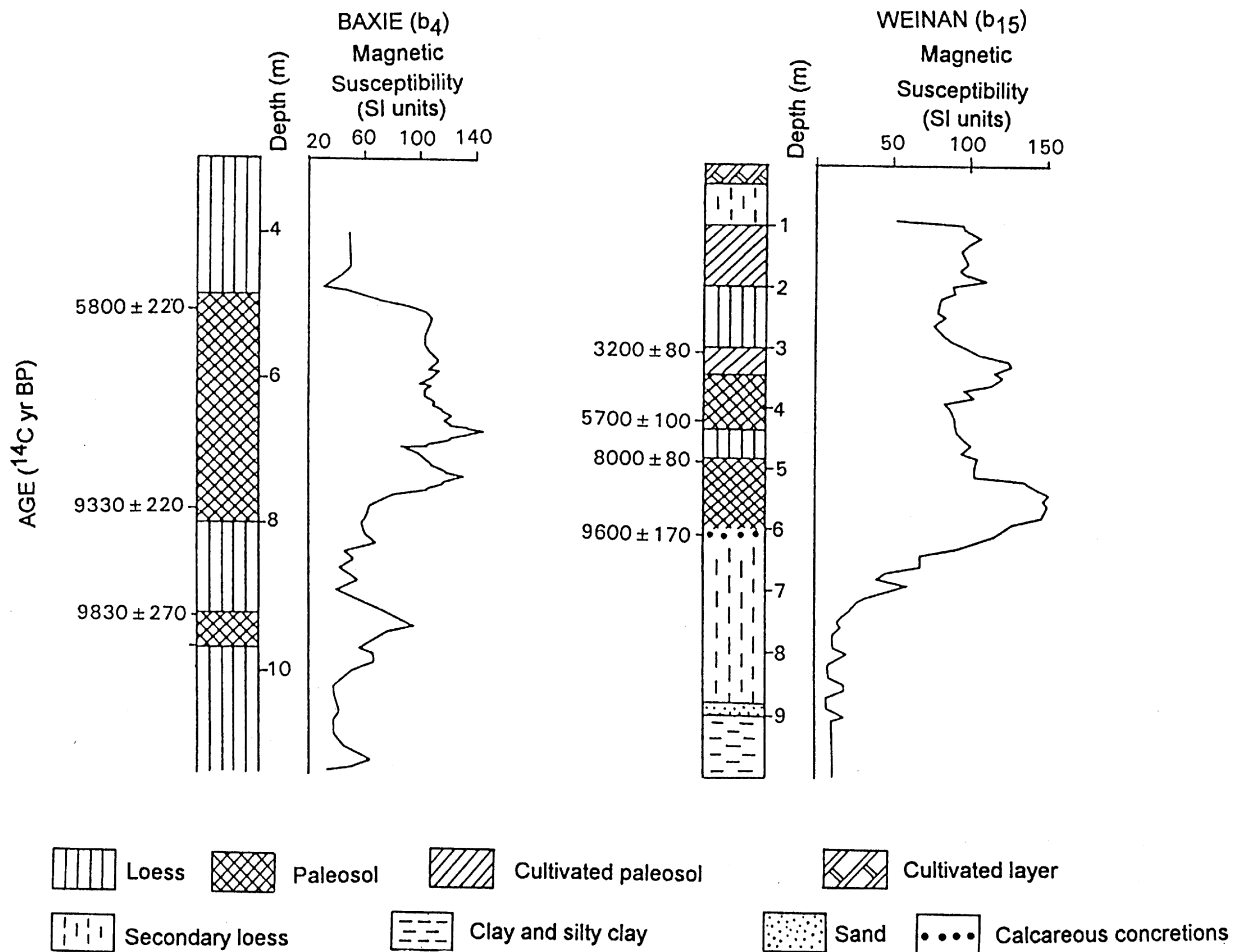


Fig. 11. Magnetic susceptibility profiles from the Southwestern and Southeastern margins of the Loess Plateau.

represented by as few as two or as many as 5 grid squares; better simulation of the monsoon-front processes will be achieved with higher-resolution models.

The precipitation peak on the central and northern Qinghai-Xizang Plateau occurred ca. 9000 cal yr BP (a deviation of 76%), a value much higher than for other regions, suggesting that the plateau is very sensitive to climatic change and exhibits a strong response.

Winkler and Wang (1993) also compared paleoclimatic proxy records from China with climate-modeling (CCM) results and came to somewhat similar conclusions. They argued that a climatic “tension zone” exists at different times of the year in central China where Arctic, central Asian, Korean, and South Pacific airstreams interact. They inferred that this zone, which is coincident with the present monsoon boundary, was displaced northward 9000 yr B.P. as the monsoonal circulation intensified. China, at that time, was wetter than now and became still wetter by 6000 yr B.P. Since then, the monsoon circulation has shifted southward, become weaker, and assumed its present pattern.

## 6. Discussion

Air temperature is widely used as the basic criterion for identifying the Holocene optimum (i.e., it is a time of optimum, or highest, temperature). However, in the East Asian monsoon region, monsoon precipitation and effective moisture (a function of precipitation, evaporation, and temperature) are the most important factors controlling biological productivity, especially in arid, semi-arid, and semi-humid areas that are sensitive to variations of the monsoon climate. As recorded by geologic and biological data, effective moisture has a strong influence on ecological environments in east-central China and determines whether the desert shrinks or advances, the level of inland lakes rises or falls, the vegetation cover becomes more or less dense, the tree limit advances or retreats, pedogenesis intensifies or weakens, and in semi-humid and humid regions, lake and swamp systems develop or vanish.

The seasonal cycle of the East Asian monsoon and the advance or retreat of its front is controlled by the seasonal cycle of insolation (Gao et al., 1962). A cycle of

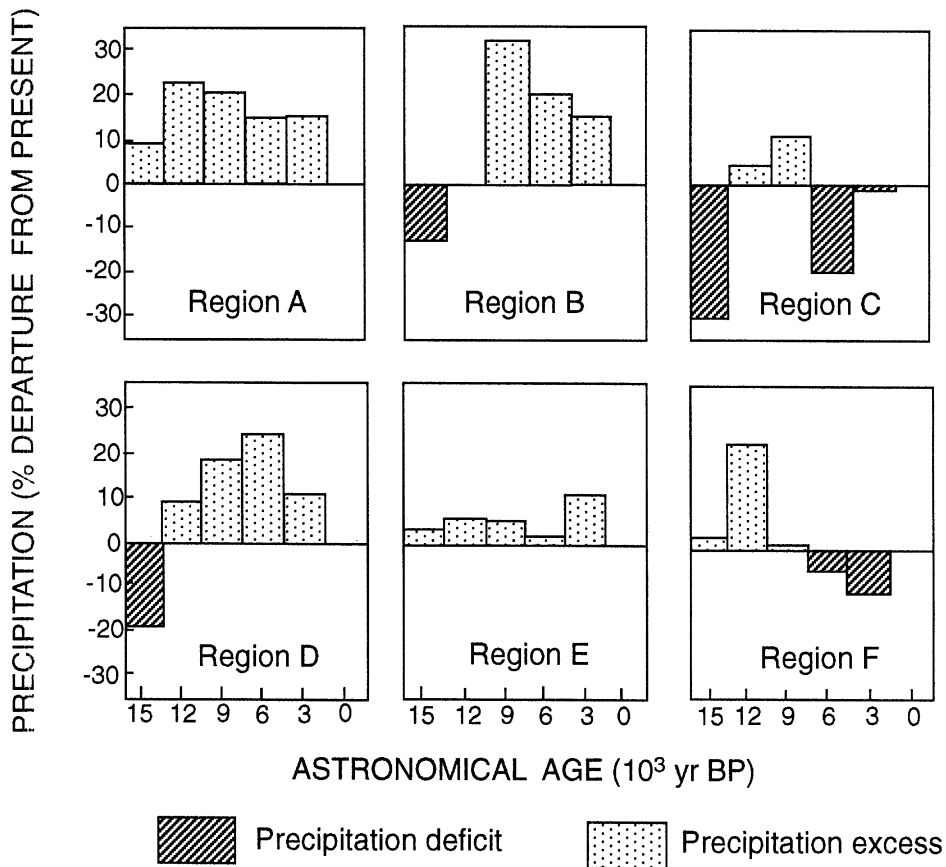


Fig. 12. July precipitation increment (% departure from present) in the Chinese monsoon region for the last 15,000 yr. Regions A, B, C, D, E, and F are the same as in Fig. 1. The precipitation values are taken from the climate-model simulations for July with CCM0, using model grid points that correspond as closely as possible to regions A–F.

Table 2  
Ages for the culmination of the Holocene optimum based on (a) <sup>14</sup>C-dated geologic evidence and (b) numerical modeling

Region	Lake-level <sup>14</sup> C age (yr BP)		Pollen <sup>14</sup> C age (yr BP)	
	Measured	Calibrated	Measured	Calibrated
<i>(a) Geologic records</i>				
Northeastern China	12,000–10,000	13,990–11,160	11,000–7000	12,920–7790
North-central China	10,000– 7000	11,160– 7790	9000	(9980
Northern east-central China	10,000– 7000	11,160– 7790	9000– 8000	9980–8830
Middle-Lower Yangtze River	8000– 7000	8820– 7790	6500	7380
Southeastern China			3000	3180
Southwestern China	12,000–10,000	13,990–11,160	9200	10,220
<i>(b) Numerical Modeling</i>				
Region	Astronomical Age (yr)	Precipitation (%)	Departure from present (mm/d)	
Northeastern China	12,000	23	0.9	
North-central China	9000	33	1.2	
Northern east-central China	9000	12	0.1	
Middle-lower Yangtze River	6000	25	0.9	
Southeastern China	3000	12	1.1	
Southwestern China	12,000	24	1.3	



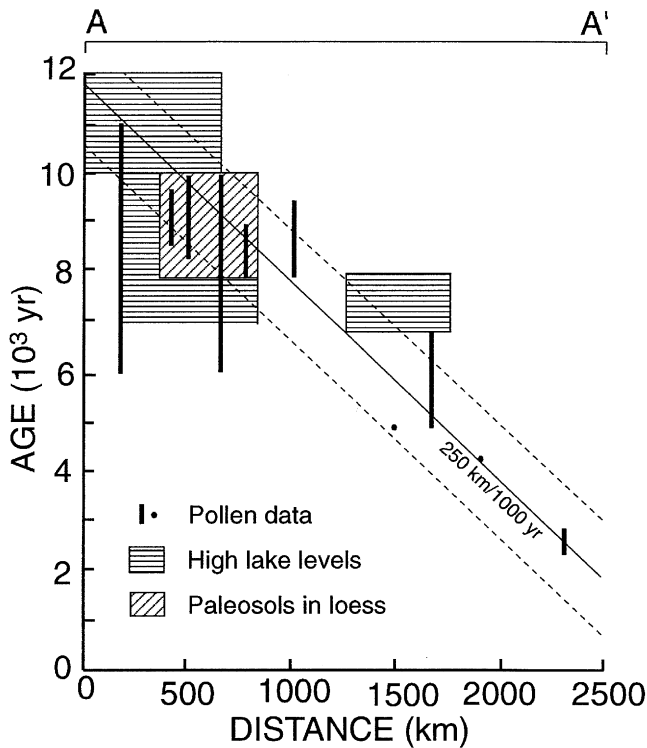


Fig. 14. Timing of the Holocene summer monsoon precipitation maximum along a transect (A–A', Fig. 13) from north-central to south-eastern China. The best-fit regression indicates a southward retreat of the belt of maximum precipitation at an average rate of 250 km/1000 yr. Dashed lines lie  $\pm 1000$  yr from the regression line.

Northern Hemisphere ice sheets delayed the development of the East Asian monsoon, but had less influence on the tropical Indian monsoon. Other important factors are the significant rise of sea level during deglaciation (Fairbanks, 1989) and the progressive warming of the high Qinghai-Xizang Plateau between ca. 15,000 and 12,000 cal yr BP, both events being favorable for the development of the Indian monsoon.

The change of climate toward wetter and warmer conditions on the Qinghai-Xizang Plateau ca. 10,000 cal yr BP is also significant. The postglacial rise in air temperature led to ablation of ice and snow on the plateau, perhaps further strengthening the Plateau monsoon. The seasonal contrast between the thermodynamics of the plateau and that of the surrounding areas is the main driving force for the Plateau monsoon (Tang, 1979). The variation of solar insolation in the Northern Hemisphere not only influences the sea-land thermodynamic contrast, but also the contrast between the plateau and the adjacent plains, which contributes to the Plateau monsoon: when the contrast increases, the converging air flow toward the plateau strengthens, and precipitation increases. Thus, during the Holocene, monsoon precipitation in China and the surrounding regions was influenced by the three relatively independent monsoon subsystems.

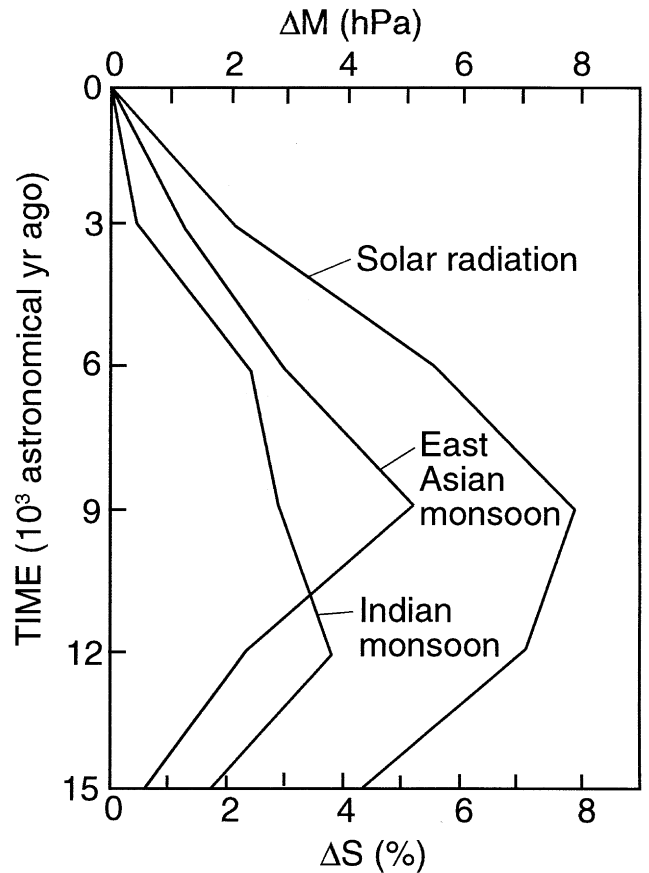


Fig. 15. Solar radiation anomaly (departure from present) ( $\Delta S$ ) compared with the East Asian monsoon index (the difference of sea-level pressure between 160° and 110°E Longitude along 25–50°N Latitude) and the tropical Indian monsoon index (the difference of sea-level pressure between ocean and land within the region 45° to 120°E Longitude and 45°N to 15°S Latitude ( $\Delta M$ (hPa); Prell and Kutzbach, 1987) at 3000-yr intervals since 15,000 astronomical yr BP. Positive values of the  $\Delta M$  index indicate generally lower pressure over land compared to the ocean. The monsoon indices are calculated from the climate-model simulations for July using CCM0.

The low-resolution CCM0 model results, although instructive, are insufficient to analyze details of the regional climate of China. For example, the model results show a systematic northward deviation from present conditions, probably due to the low horizontal resolution of the model, the simplified parameterizations of physical processes, and the simplification of plateau relief. The seasonal variation of the East Asian monsoon is not simulated by this version of the model, and the selected values of sea-surface temperature and soil humidity may not be sufficiently accurate. Also not taken into account is the changing concentration of  $\text{CO}_2$  and other trace gases in the atmosphere. More-recent simulations incorporate seasonal changes, mixed-layer ocean changes, and  $\text{CO}_2$  changes (Kutzbach et al., 1998).

At present, the resolution of geologic records and numerical models is too low to provide detailed and precise

analysis of the complex East Asian paleomonsoon system. In each case, improved resolution is a high-priority research target. For example, models are needed that incorporate the interrelationship between continental hydrology and the atmosphere, as well as the coupling of land and ocean. This work with improved models is now in progress (Kutzbach and Gallimore, 1988; Gallimore and Kutzbach, 1989; Kutzbach et al., 1996; Kutzbach and Liu, 1997; Kutzbach et al., 1998). Geologic climate-proxy records require better and more plentiful age control, and improved means of quantifying paleoclimatic parameters.

Reconstruction of the Holocene history of the East Asian monsoon raises an important question: How might the pattern and intensity of summer monsoon precipitation in central and eastern China change in the coming decades in response to the increasing concentration of anthropogenically generated greenhouse gases in the atmosphere? More specifically, does the Holocene pattern of climate change in response to orbital forcing provide insight into the processes that might influence climate variations in the East Asian monsoon region in the near future? Whether the response might be regionally rapid, or far slower and therefore diachronous (as during the Holocene), is of obvious interest. An additional question concerns whether higher-frequency climate variability, similar to that recently recognized in the North Atlantic paleoclimate records (e.g., Bond et al., 1997), influenced the Holocene monsoon region of China. Such variability, superimposed on the longer-term trend reported here, is evident in many of the records we have examined (e.g., Figs. 6, 7, 9 and 10). Further high-resolution stratigraphic studies may help us to understand whether the Holocene climate of China was unique to this monsoon region or was closely in step with that of other regions in the Northern Hemisphere.

## 7. Conclusions

Geologic data and numerical modeling are consistent in showing that the Holocene optimum, as defined by peak precipitation or effective moisture, is diachronic in central and eastern China, i.e., it appears earlier in the north and northeast and later in the south and southeast, and is related to a general weakening and southward retreat of the East Asian summer monsoon since ca. 9000 yr BP.

## Acknowledgements

This research was supported by the U.S. National Science Foundation, the National Science Foundation of China, the Chinese Academy of Sciences, and the SSTC.

Wang Jian, Xiao Jiayi, Liu Junfeng, and Lu Jijun assisted in the collection and analysis of data. We are grateful to Patrick Bartlein and Kam-biu Liu for their helpful critiques of the manuscript.

## References

- An, Zhisheng, Liu, Tungsheng, Lu, Yanchou, Porter, S.C., Kukla, G., Wu, Xihao, Hua, Yingming, 1990a. The long term paleomonsoon variation recorded by the loess-paleosol sequence in central China. *Quaternary International* 7/8, 91–95.
- An, Zhisheng, Wu, Xihao, Lu, Yanchou, Zhang, De'er, Sun, Xiangjun, Dong, Guangrong, 1990b. A preliminary study on the paleoenvironment change of China during the last 20,000 years. In: Liu, Tungsheng (Ed.), *Loess, Quaternary Geology and Global Change*. Science Press, Beijing, pp. 1–26 (in Chinese).
- An, Zhisheng, Kukla, G.J., Porter, S.C., Xiao, Jule, 1991a. Magnetic susceptibility evidence of monsoon variation on the Loess Plateau of central China during the last 130,000 years. *Quaternary Research* 36, 29–36.
- An, Zhisheng, Wu, Xihao, Wang, Pinxian, Dong, Guangrong, Sun, Xiangjun, Zhang, De'er, Lu, Yanchou, Zheng, Shaohua, Zhao, Songling, 1991b. The paleomonsoon during the last 130,000 years in China. *Science in China, Series B* 34 (8), 1007–1024.
- An, Zhisheng, Porter, S.C., Zhou, Weijian, Lu, Yanchou, Donahue, D., Head, J., Wu, Xihao, Ren, Jianzhan, 1993. Episode of strengthened summer monsoon climate of Younger Dryas age on the Loess Plateau of central China. *Quaternary Research* 39, 45–54.
- Bates, R.L., Jackson, J.A., (Eds.), 1987. *Glossary of Geology*. American Geological Institute, Alexandria, VA, 788 p.
- Bond, G., Showers, W., Cheseby, M., Lotti, R., Almasi, P., deMenocal, P., Priore, P., Cullen, H., Hajdas, I., Bonani, G., 1997. A pervasive millennial-scale cycle in North Atlantic Holocene and glacial climates. *Science* 278, 1257–1266.
- Chen, Fahu, Li, Jijun, Zhang, Weixin, Pan, Baotian, 1991a. The loess profile of south bank, climate information and lake-level fluctuation of Qinghai Lake during the Holocene. *Scientia Geographica Sinica* 11 (1), 76–85 (in Chinese).
- Chen, Fahu, Li Jijun, Zhang, Weixin, 1991b. Loess stratigraphy of the Lanzhou profile and its comparison with deep-sea sediment and ice core record. *GeoJournal* 24 (2), 201–209.
- COHMAP Members, 1988. Climatic changes of the last 18,000 years: observations and model simulation. *Science* 241, 1043–1052.
- Cui, Haiting, Kong, Zhaochen, 1992. A preliminary analysis about the climatic fluctuation of Holocene. Megathermal in the Central and Eastern parts of Inner Mongolia. In: Shi, Y.F. (Ed.), *The climate and environment of Holocene Megathermal in China*. China Ocean Press, Beijing pp. 72–79 (in Chinese).
- Cui, Zhijiu, Song, Changqing, 1992. The periglacial phenomenon and environmental evolution during Holocene in Daqingshan (mountain). *Glacier and Permafrost* 14, 325–331 (in Chinese).
- Du, Naiqiu, Kong, Zhaochen, Shan, Fashou, 1989. A preliminary investigation on the vegetational and climatic changes since 11,000 years in Qinghai Lake. An analysis based on palynology in core QH85-14C. *Acta Botanica Sinica* 31, 803–814 (in Chinese).
- Editorial Committee of Studies on Poyang Lake, 1987. *Study on Poyang Lake*. Shanghai Press of Science and Technology, Shanghai pp. 63–69 (in Chinese).
- Fairbanks, R.K., 1989. A 17,000-year glacio-eustatic sea level record: influence of glacial melting rates on the Younger Dryas event and deep-ocean circulation. *Nature* 342, 637–642.
- Gallimore, R.G., Kutzbach, J.E., 1989. Effects of soil moisture on the sensitivity of a climate model to earth orbital forcing at 9000 yr BP. *Climatic Change* 14, 175–205.

- Gao, Youxi, 1962. Some Problems on East-Asia Monsoon. Science Press, Beijing, pp. 49–63 (in Chinese).
- Gao, Youxi, Xiao, Xuying, Guo, Qiyun, Zhang, Miling, 1962. The subdivision of monsoonal regions and the regional climates in China. In: Gao, Youxi (Ed.), Some problems on East-Asia Monsoon. Science Press, Beijing, pp. 49–63 (In Chinese).
- Gasse, F., Arnold, M., Fontes, J.C., Fort, M., Gilbert, E., Huc, A., Li, Bingyan, Li, Yuanfang, Liu, Qing, Mélières, F., Van Campo, E., Wang, Fubao, Zhang, Qingsong, 1991. A 13,000-year climate record from western Tibet. *Nature* 353, 742–745.
- Geng, Kan, 1988. The geomorphologic features and evolution of the Holocene lakes in Dalainoer area, Inner Mongolia. *Bulletin of Beijing Normal University (Natural Sciences)* 4, 94–100 (in Chinese).
- Gu, Zhaoyan, Liu, Jiaqi, Yuan, Baoyin, Liu, Tungsheng, Liu, Rongmo, Liu, Yu, Zhang, Guangyu, 1993. The evolution of the Qinghai-Xizang Plateau monsoon; evidence from the geochemistry of the sediments in Seling Co Lake. *Chinese Science Bulletin* 38, 61–64 (in Chinese).
- Harrison, S.P., Digerfeldt, G., 1993. European lakes as palaeohydrological and palaeoclimatic indicators. *Quaternary Science Reviews* 12, 233–248.
- Hunag, Qi, Chai, Biqing, Yu, Jungqing, 1980. The  $^{14}\text{C}$  dating and the Psedimentary cycle in the saline lakes on the Qinghai-Xizang Plateau. *Chinese Science Bulletin* 25, 990–994 (in Chinese).
- Institute of Geochemistry, Chinese Academy of Sciences, 1977. Environmental changes in southern Liaoning Province during the last 10,000 years. *Scientia Sinica, Series B* 22, 603–614 (in Chinese).
- Jarvis, D.I., 1993. Pollen evidence of changing Holocene monsoon climate in Sichuan Province, China. *Quaternary Research* 39, 325–337.
- Kelts, K., Zao, C.K., Lister, G., Hong, G.Z., Niessen, F., Bonani, G., 1989. Geological fingerprints of climatic history; a cooperative study of Qinghai Lake, China. *Ecologiae Geology* 82, 167–182.
- Kutzbach, J.E., Bonan, G., Foley, J., Harrison, S.P., 1996. Vegetation and soil feedbacks on the response of the African monsoon to orbital forcing in the early to middle Holocene. *Nature* 384, 623–636.
- Kutzbach, J.E., Gallimore, R.G., 1988. Sensitivity of a coupled atmosphere/mixed-layer ocean model to changes in orbital forcing at 9000 yr BP. *Journal of Geophysical Research* 93, 803–821.
- Kutzbach, J., Gallimore, R., Harrison, S., Behling, P., Selin, R., Laarif, 1998. Climate and biome simulations for the past 21,000 years. *Quaternary Science Reviews*, 17, 473–506
- Kutzbach, J.E., Guetter, P.J., 1986. The influence of changing orbital parameters and surface boundary conditions on climate simulation for the past 18,000 years. *Journal of Atmospheric Science* 43, 1726–1759.
- Kutzbach, J.E., Liu, Z., 1997. Response of the African monsoon to orbital forcing and ocean feedbacks in the middle Holocene. *Science* 278, 440–443.
- Lau, K.M., Yang, G.J., Sheu, S.H., 1988. Seasonal and intraseasonal climatology of monsoon rainfall over East Asia. *Monthly Weather Review* 116, 18–37.
- Li, Huazhang, Liu, Qingsi, Wang, Jiaxing, 1992a. Study on the evolution of Huangqihai and Daihai lakes in the Holocene on the Inner Mongolia Plateau. *Journal of Lake Sciences* 4, 31–39 (in Chinese).
- Li, Pingri, Zheng, Jiansheng, Fang, Guoxiang, (1991). *Quaternary Geology in the Guangzhou area*. Printing House of the Huanan University of Science and Technology, pp. 53–81 (in Chinese).
- Li, Wenyi, Liang, Yulian, 1985. Vegetation and environment of the hypsithermal interval of Holocene in the eastern Heibei Plain. *Acta Botanica Sinica* 27, 640–651 (in Chinese).
- Li, Wenyi, Liu, Guangxiu, Zhou, Mingming, 1992b. The vegetation and climate of the Holocene Hypsithermal in Northern Hubei Province. In: Shi, Y.F. (Ed.), *The Climate and environments of Holocene Megathermal in China*. China Ocean Press, Beijing: pp. 94–99 (in Chinese).
- Li, Xiaoqiang, 1991. A preliminary study on the evolution of the environment of the Jinbian district, Sha'anxi, for the last 12,500 years. Unpub. Master's Thesis, Academia Sinica (in Chinese).
- Lin, Shaomeng, 1987. The vegetation history from the late Pleistocene to Holocene at Eryuan, Yunnan Province. In: Sino-Australia Cooperative Group (Ed.), *Contributions to the Quaternary Symposium*. Science Press, Beijing, pp. 56–67 (in Chinese).
- Lin, Shuji, Zheng, Honghan, 1987. Evolution of Caohai Lake. Guizhou People's Press, Guiyang: pp. 7–38 (in Chinese).
- Liu, J., 1989. Vegetational and climatic changes at Gushantun Bog in Jilin, NE China since 13,000 a BP. *Acta Palaeontologica Sinica* 28, 240–248 (in Chinese).
- Liu, Kam-biu, 1988. Quaternary history of the temperate forests of China. *Quaternary Science Reviews* 7, 1–20.
- Liu, Kam-biu, Qiu, Hongli, 1994. Late Holocene pollen records of vegetational changes in China: climate or human disturbance. *Tao* 5, 393–410.
- Liu, Kam-biu, Sun, Shuncai, Jiang, Xinhe, 1992. Environmental change in the Yangtze River Delta since 12,000 years B.P. *Quaternary Research* 38, 32–45.
- Nanjing Institute of Geography, and Limnology (CAS), 1989. *Environments and Sedimentation of Fault Lake, Yunnan Province*. Science Press, Beijing (in Chinese).
- Pitcher, E.J., Malone, R.C., Ramanathan, V., Blackman, M.L., Pury, K., Bourke, W., 1983. January and July simulations with a spectral general circulation model. *Journal of Atmospheric Science* 40, 580–604.
- Porter, S.C., An, Zhisheng, 1995. Correlation between climate events in the North Atlantic and China during the last glaciation. *Nature* 375, 305–308.
- Prell, W.L., Kutzbach, J.E., 1987. Monsoon variability over the past 150,000 years. *Journal of Geophysical Research* 92, 8411–8425.
- Ramage, C.S., 1987. *Phenomenon of Monsoon* (translated by Feng, Xiucao). Science Press, Beijing (in Chinese).
- Ruddiman, W.F., Kutzbach, J.E., 1991. Plateau uplift and climatic change. *Scientific American* 264 (3), 66–75.
- Shi, Yafeng, Kong, Zhangchen, Wang, Suming, Tang, Lingyu, Wang, Fubao, Chen, Yaodong, Zhao, Xitao, Zhang, Peiyuan, Shi, Saohua, 1992. Basic feature of climates and environments during the Holocene Megathermal in China. *Science in China, B Series* 35, 1300–1308 (in Chinese).
- Song, Xieliang, 1994. *Palaeolimnological Studies on the Limestone District in Central Yunnan*. Science and Technology Press, Beijing (in Chinese).
- Street, F.A., Grove, A.T., 1979. Global map of lake-level fluctuations since 30,000 yr B.P.. *Quaternary Research* 12, 83–118.
- Street-Perrott, F.A., Harrison, S.P., 1984. Temporal variation in lake levels since 30,000 yr B.P. — An index of the global hydrological cycle. In: Hansen, J.E., Takahashi, T. (Eds.), *Climate Processes and Climate Sensitivity*, Geophysical Monograph Series, Vol. 29. American Geophysical Union, Washington, DC, pp. 118–129.
- Stuiver, M., Reimer, P.J., 1993. Extended  $^{14}\text{C}$  data base and revised CALIB 3.0  $^{14}\text{C}$  age calibration program. *Radiocarbon* 35, 215–230.
- Sun, Dapeng, 1990. The soda Lakes on the Inner Mongolia Plateau, China. *Oceanologia et Limnologia Sinica* 21, 44–53 (in Chinese).
- Sun, Donghai, Shaw, John, An, Zhisheng, Chen, Minyang, Yue, Leping, 1998. Magnetostratigraphy and paleoclimatic interpretation of a continuous 7.2 Ma Late Cenozoic eolian sediments from the Chinese Loess Plateau. *Geophysical Research Letters* 25, 85–88.
- Sun, Jianzhong, Zhao, Jinbo, 1991. Quaternary of the Loess Plateau. Science Press, Beijing, pp. 186–205 (in Chinese).
- Sun, Shuncai, Wu, Yifan, 1987a. The formation and evolution of Taihu Lake and sedimentation. *Science in China, Series B* 30, 1329–1339 (in Chinese).
- Sun, Xiangjun, Wu, Yushu, 1987b. Holocene vegetation history and environmental changes of the Dianchi Lake area, Yunnan Province. *Proceedings of China-Australia Academia Symposium*

- on Quaternary Geology. Science Press, Beijing, pp. 28–41 (in Chinese).
- Sun, Xiangjun, Yuan, Shaomin, 1990. Pollen data and evolution of the vegetation for the last 10,000 years in Jinchuan basin, Jiling Province. In: Loess, Quaternary Geology, and Global Change, Vol. 2. Science Press, Beijing, pp. 46–47 (in Chinese).
- Tan, Qixiang, 1980. Yunmen and Yunmence. Bulletin of Fudan University (Special Issue on Historical Geography) 1911 (in Chinese).
- Tang, Lingyu, Shen, Caiming, 1992. The vegetation and climates of the Holocene Megathermal in northern Jiangsu Province. In: Shi, Y.F. (Ed.), The climates and environments of the Holocene Megathermal in China. Chinese Ocean Press, Beijing pp. 80–93 (in Chinese).
- Tang, Lingyu, Shen, Caiming, Zhao, Xitao, Xiao, Jiayi, Yu, Ge, Han, Huiyou, 1993. The vegetation and the climate during the last 10,000 yr. BP in Qingfeng profile of Jianghu, Jiangsu. Science in China 23, 637–643.
- Tang, Maocang, 1979. The average characteristics of the Plateau monsoon climate. Acta Geographica 34 (in Chinese).
- Tao, S.Y., Chen, L.X., 1987. A review of recent research on the East Asian summer monsoon in China. In: Chang, C.P., Krishnamurti, T.N. (Eds.), Oxford University Press, Oxford, pp. 60–92.
- Wang, Suming, Ji, Lei, Yang, Xiangdong, Xue, Bin, Ma, Yan, Hu, Shouyun, 1994. Record of Younger Dryas event in the lacustrine in Zhalainguoer of Inner Mongolia. Chinese Science Bulletin 39, 348–351 (in Chinese).
- Wang, Suming, Wu, Ruijin, Jiang, Xinhe, 1990a. Environmental evolution and paleoclimate of Daihai Lake, Inner Mongolia, since the last glaciation. Quaternary Sciences 3, 223–232 (in Chinese).
- Wang, Suming, Yu, Yuansheng, Wu, Ruijin, Feng, Min, 1990b. Daihai Lake environmental evolution and climate change. Printing House of University of Science and Technology of China, pp. 117–182 (in Chinese).
- Williamson, D.L., 1983. Description of NCAR Community Climate Model (CCMOB), NCAR Technical Note, NCAR/TN-210 + STR, Boulder, Colorado, 88 pp.
- Winkler, M.G., Wang, P.K., 1993. The late Quaternary vegetation and climate of China. In: Wright Jr, H.E., Kutzbach, J.E., Webb III, T., Ruddiman, W.F., Street-Perrott, F.A., Bartlein, P.J. (Eds.), Global Climates since the Last Glacial Maximum. University of Minnesota Press, Minneapolis, pp. 221–264.
- Wu, Zhengyi, et al. 1980. Vegetation of China. Science Press, Beijing, pp. 1–1144.
- Xia, Yumei, 1988. Preliminary study on vegetational development and climatic changes in the Sanjiang Plain in the last 12,000 years. Scientia Geographica Sinica 8, 240–249 (in Chinese).
- Xu, Qin Hai, Chen, Shuyin, Kong, Zhaochen, Du, Naiqiu, 1988. Preliminary study of vegetation succession and climatic change since the Holocene in the Baiyangdian Lake district. Acta Phytocologica et Geobotanica Sinica 12, 143–151 (in Chinese).
- Xu, Xin, Zhu, Minglun, 1984. Changes in the vegetation and environment in the Zhenjiang region since 15,000 years ago. Acta Geographica Sinica 39, 277–284.
- Xue, Bin, Wang, Suming, 1994. The evolutionary and monsoonal processes in the lakes and swamps of central and eastern China since the last 12,000 years. Journal of Hehai University 22, 46–51.
- Yang, Huairan, 1989. Future global change and the Neo-hypsithermal climate. Studies on Climatology. Meteorological Press, Beijing: pp. 290–301 (in Chinese).
- Yuan, Baoyin, 1988. Geological significance of the climatic geomorphology of the Late Pleistocene in North China. Acta Scientiarum Naturalium Universitatis Pekinensis 24, 235–244 (in Chinese).
- Zhang, Jiachen, Lin, Zhiguang, 1985. Climate of China. Shanghai Press of Science and Technology, Shanghai, pp. 246–268.
- Zhang, Xiaoyang, 1991. The formation and evolution of Dongting Lake and delta deposit. M.S. Thesis, Nanjing Institute of Geography (in Chinese).
- Zhou, Kunshu, Chen, Shuomin, Chen, Chenghui, Ye, Yongying, Liang, Xiulong, 1984. Pollen analysis of the Holocene in North China and paleo-environments. In: Spore-pollen analysis of the Quaternary and paleo-environments. Science Press, Beijing, pp. 25–53 (in Chinese).
- Zhou, Mingfu, Shen, Chengde, Huang, Baolin, Qiao, Yulou, 1992.  $^{14}\text{C}$  chronology of the variation of Fuxian Lake and the neotectonic movement of Chengjiang basin in Yunnan Province during the last 50 ka. In: Loess, Quaternary Geology, and Global Change, 3. Science Press, Beijing, pp. 155–160 (in Chinese).
- Zhou, Weijian, An, Zhisheng, 1991.  $^{14}\text{C}$  chronology of Loess Plateau in China. In: Liu, Tungsheng (Ed.), Quaternary Geology and Environment in China. Science Press, Beijing, pp. 192–200 (in Chinese).
- Zhu, Haihong, 1989. Lacustrine Environment and Sediments of the Yunnan Fault-Downwarped Lakes. Science Press, Beijing (in Chinese).